

Master of Science Thesis in Electrical Engineering
Department of Electrical Engineering, Linköping University, 2016

Modeling and Estimation of Long Route EGR Mass Flow in a Turbocharged Gasoline Engine

Erik Klasén

Master of Science Thesis in Electrical Engineering

Modeling and Estimation of Long Route EGR Mass Flow in a Turbocharged Gasoline Engine

Erik Klasén

LiTH-ISY-EX--16/4985--SE

Supervisor: **Marcus Rubensson**
Volvo Car Corporation
Sebastian Krause
Volvo Car Corporation
Kristoffer Ekberg
ISY, Linköping University

Examiner: **Lars Eriksson**
ISY, Linköping University

*Division of Vehicular Systems
Department of Electrical Engineering
Linköping University
SE-581 83 Linköping, Sweden*

Copyright © 2016 Erik Klasén

Abstract

Due to the continuous work in the automobile industry to reduce the environmental impact, reduce fuel consumption and increase efficiency, new technologies need to be developed and implemented in vehicles. For spark ignited engines, one technology that has received more attention in recent years is long route Exhaust Gas Recirculation (EGR), which means that exhaust gases after the turbine are transported back to the volume before the compressor in the air intake system of the engine.

In this work, the components of the long route EGR system is modeled with mean value engine models in Simulink, and implemented in a existing Simulink engine model. Then different methods for estimating the mass flow over the long route EGR system are compared, and the transport delays for the recirculated exhaust gases in the engines air intake system are modeled. This work is based on measurements done on an engine rig, on which a long route EGR system was installed. Finally, some ideas on how a long route EGR system on a gasoline engine can be controlled are presented based on the results in this thesis work.

Acknowledgments

At Volvo Cars Corporation, I would like to thank my supervisors Sebastian Krause and Marcus Rubensson for all the help and input I have received during my work with the master thesis. I also would like to thank Anna Hägg and Fredrik Wemmert at Volvo Cars Corporation.

At the Division of Vehicular Systems at Linköping University, i would like to thank Tobias Lindell for all the help with the engine rig and measurements. I also would like to thank my supervisor at the university, Kristoffer Ekberg, for the help during my thesis work, and my examiner Lars Eriksson for the knowledge I have gained from his courses in this area. And thanks to Peter Möller at *FunMat* for the cooperation with the SiC-FET oxygen sensor.

Linköping, June 2016
Erik Klasén

Contents

Notations	ix
1 Introduction	1
1.1 Problem formulation	2
1.2 Literature review	3
1.3 Delimitations	5
2 System Description	7
2.1 Engine data	7
2.2 Silicon carbide field effect transistor oxygen sensor	8
2.3 Long route EGR system	8
3 Long Route EGR System Modeling and Estimation Fundamentals	11
3.1 Modeling method	11
3.1.1 Flow restrictions	11
3.1.2 Control volumes	12
3.1.3 Temperature exchange	13
3.1.4 Gas mixture	13
3.2 Modeling the components of the long route EGR system	15
3.2.1 Modeling the three-way catalyst	15
3.2.2 Modeling long route EGR intercooler	17
3.2.3 Modeling the long route EGR valve	19
3.2.4 Gas mixture in air intake control volumes	20
3.3 Estimating mass flow in the long route EGR system	21
3.3.1 Estimating mass flow by measuring the oxygen	21
3.3.2 Estimating mass flow by measuring the pressure difference over the long route EGR valve	22
3.3.3 Estimating mass flow from the volumetric efficiency model	22
3.4 Estimating and modeling transport delays for recirculated gases .	22
4 Results	31
4.1 Model validation	32
4.1.1 Catalyst	32

4.1.2	Long route EGR intercooler	35
4.1.3	Long route EGR valve	38
4.2	Estimation of long route EGR mass flow	39
4.3	Measurement with the SiC-FET oxygen sensor	39
4.4	Estimating and modeling transport delays for recirculated gases	41
4.4.1	Time estimation models	41
4.4.2	Time delay simulations in Simulink	44
5	Discussion and Conclusion	53
5.1	Model of the long route EGR system	53
5.2	Different methods of estimating the mass flow over the long route EGR circuit	54
5.3	Proposed control strategy for the long route EGR system	55
5.4	Future work	56
	Bibliography	57

Notations

VARIABLES AND PARAMETERS

Notation	Description
ε	Long route EGR intercooler efficiency coefficient [-]
γ	Ratio of specific heats [-]
λ	Air/Fuel-ratio [-]
c_p	Specific heat capacity at constant pressure [J/kgK]
c_v	Specific heat capacity at constant volume [J/kgK]
\dot{m}_{air}	Air mass flow through air filter [kg/s]
\dot{m}_{cyl}	Air mass flow into cylinders [kg/s]
\dot{m}_{EGR}	Mass flow over the LR EGR circuit [kg/s]
N	Engine speed [rpm]
p_{amb}	Ambient air pressure [Pa]
p_{bComp}	Pressure between air filter and turbo compressor [Pa]
p_{ic}	Intercooler pressure [Pa]
p_{im}	Intake manifold pressure [Pa]
p_{cyl}	Cylinder pressure [Pa]
p_{em}	Exhaust manifold pressure [Pa]
p_{bCat}	Pressure after turbine before the first catalyst [Pa]
p_{cat}	Pressure between first and second catalyst [Pa]
p_{aEGRic}	Pressure between LR EGR cooler and LR EGR valve [Pa]
p_{es}	Downstream pressure in exhaust system [Pa]

VARIABLES AND PARAMETERS

Notation	Description
R_{air}	Gas constant for air [J/kgK]
R_{exh}	Gas constant for exhaust gases [J/kgK]
T_{amb}	Ambient air temperature [K]
T_{af}	Temperature after air filter [K]
T_{mix}	Temperature after LR-EGR mixing point [K]
T_{bIC}	Temperature between compressor and intercooler [K]
T_{bTh}	Temperature between intercooler and throttle [K]
T_{im}	Temperature in intake manifold [K]
T_{em}	Temperature in exhaust manifold [K]
T_{bCat}	Temperature between turbine and first catalyst [K]
T_{cat}	Temperature between catalysts [K]
T_{bEGRic}	Temperature before LR-EGR intercooler [K]
T_{aEGRic}	Temperature after LR-EGR intercooler [K]
T_{cool}	Coolant temperature in LR-EGR intercooler [K]
T_{es}	Downstream temperature in exhaust system [K]
u_{EGR}	LR-EGR valve control signal [-]
$X_{O,EGR}$	Fraction of oxygen in the recirculated exhaust gases [-]
$X_{O,air}$	Fraction of oxygen in the ambient air [-]
X_B	Burned gas fraction in gas [-]

SHORTENINGS

Shortening	Meaning
SI Engine	Spark Ignited Engine
ECU	Engine Controller Unit
LR EGR	Long Route Exhaust Gas Recirculation
iVVT	Inlet Variable Valve Timing
eVVT	Exhaust Variable Valve Timing
SiC-FET	Silicon Carbide Field Effect Transistor

1

Introduction

For internal combustion engines in cars, Exhaust Gas Recirculation (EGR) has been widely used for decades, see Hawley et al. [3], to reduce the emission of nitrogen oxides NO_x , Heywood [4]. One way to recirculate the exhaust gases is called long route EGR, or sometimes low pressure EGR, where a part of the exhaust gases after the turbochargers turbine are transported back to the volume before the compressor. Due to the continuous work in the automobile industry to reduce the environmental impact, reduce fuel consumption and meet new regulations. Therefore, the long route EGR system on turbocharged gasoline engines has started to gain more attention in recent time.

In this thesis, the Long Route EGR system on a gasoline engine is further studied by:

- Analysing and comparing different methods to estimate the gas composition after mixing the fresh air with the exhaust gases in the air intake
- Model the time delay for the recirculated exhaust gases on the air intake side of the engine
- Modify and parametrize existing engine simulation models for a long route EGR system
- Proposing a control strategy based on the results

To be able to collect data for this work, a long route EGR system was installed on an engine in a test cell. In section 2, long route EGR system is further described.

1.1 Problem formulation

Since the spark ignited gasoline engine has to be run at a more narrow air/fuel-ratio compared to diesel engines, EGR systems on turbocharged SI engines often become more complex to control than diesel engines. The exhaust gases that are recirculated into the intake manifold contain less oxygen. To maintain a stoichiometric combustion, and avoid misfire and knock, this needs to be accounted for in the control system. This can be achieved by estimating the long route EGR mass flow. To perform the estimation and be able to control the long route EGR system, several questions need to be answered:

- How can the long route EGR mass flow be estimated and how does the different methods perform?
- Which transport delays occurs for the recirculated gases between the long route EGR valve and cylinders?
- How can the transport delays from the long route EGR vale to the cylinders be modeled?

For a vehicle manufacturer, the information of how well different methods of estimating the gas composition performs, can be useful when deciding which method that should be used in a production vehicle. The different methods may differ in parameters such as reliability, accuracy and control performance of the engine. If the methods differ significant in production cost due to different sensor prices, that factor will certainly play a big role as well, if the vehicle is planned to be manufactured in large volumes.

Good knowledge of the transport delays facilities the decision-making of where to place eventual sensors. For example, if the amount of recirculated gas is measured or estimated just before the engine, the information provided by the sensor might be possible to use when controlling the ignition or an internal EGR system. On the other hand, the long route EGR valve might be easier to control if the sensor is placed closer to the EGR valve, to avoid the time delay caused by gas transportation time from the EGR valve to the sensor.

For developing and evaluating control algorithms for a system, a simulation model of the system that is about to be controled is a valuable tool. This thesis also treats the following questions:

- How can a long route EGR system be modeled and implemented in an existing simulation model of an engine in Simulink?
- How can the transport delay models be implemented in the simulation model of the engine with the long route EGR system implemented?

1.2 Literature review

Previous studies on EGR system on SI engines have been made several times before. Wei et al. [17] investigates the effects on performance, emissions and knock suppression on when recirculating both hot and cold exhaust gases on a SI engine. One of their conclusions was that recirculated cooled exhaust gases can inhibit knock and reduce emissions. Luján et al. [8] investigated a low pressure EGR system on a turbocharged direct injected SI engine at 2000 rpm at part load and high load. At part load, they found that the fuel consumption could be decreased by better combustion phasing, reduced pumping losses and less heat losses through the cylinder walls. The NO_x and CO and soot emissions were also reduced. The results at high load were similar to the results at partial load, but with a large decrease of NO_x , CO , HC and soot after the catalyst due to elimination of the fuel enrichment cooling strategy.

Siokos et al. [15] made a similar study on a Low Pressure EGR system on a TCDI SI Engine. This study also showed decreased pumping and heat transfer losses, increased knock suppression and increased fuel efficiency by eliminating fuel enrichment.

There are also several studies made on different EGR systems on diesel engines, which to some extent is relevant for EGR systems on SI engines. Oldřich et al. [11] investigated four different EGR systems (including one LR EGR system similar to this study) and described how each system affected the pumping work and fuel consumption. Park and Bae [12] investigates how the proportion of recirculated exhaust gases on long and short route EGR systems affects the emissions, fuel consumption and combustion.

The work mentioned above clearly shows that a long route EGR system for a turbocharged SI engine can yield several advantages in performance, fuel efficiency and decreased emissions, which makes further studies in the subject interesting. One of the main issues with a long route EGR system on a turbocharged SI engine is to estimate the mass flow of the recirculated exhaust gases and develop a control strategy that fits for production engines. When developing a control strategy, simulation models are valuable tools. Previous studies on modeling and simulation of EGR systems in Simulink have been made at the *Division of Vehicular Systems at Linköping University*. Qiu [13] modeled and simulated both long and short route EGR systems for spark ignited engines in Simulink, and Wahlström and Eriksson [16] have modeled an EGR system in Simulink for a diesel engine. This article describes how the temperature, pressure and the oxygen fraction is affected in the volume where the EGR gases are mixed with the fresh air, which can be useful when modeling the Long Route EGR system in Simulink. The long route EGR system can also be combined with internal EGR on engines with variable cam phasing (iVVT and eVVT). Öberg [10] describes how the area around the cylinders can be modeled on an engine with variable

cam phasing.

Liu and Pfeiffer [6] have analysed the accuracy of an estimation method for the EGR flow in a long route EGR system on a turbocharged SI engine. The results shows that the estimation error increases with low pressure differences over the long route EGR valve at 1250 and 1500 rpm. The estimation error became larger at 1250 rpm compared to 1500 rpm.

Lee et al. [5] estimates the recirculated mass flow from the long route EGR in a diesel engine. The mass flow is estimated with only production sensors by using an adaptive observer with an updating rule derived from the Lyapunov stability theory.

When modeling the exhaust gas concentration on the air intake side of the engine in Simulink, the time delay for the gas transportation has to be taken into account if the model is going to be used for investigating different control strategies. The time delay for the gas transportation will most likely vary with the mass flow and density, which is to be investigated. One method to model that behaviour in Simulink might be to use a time delay block with a time constant that depends on mass flow and density. If the simulation results from that method would be insufficient, one interesting method to investigate would be to model the pipes in which the gases are transported with one dimensional computational fluid dynamic (CFD). If the gas transportation needs to be modeled with one dimensional CFD, the work made by Renberg [14] examines one dimensional CFD modeling of a turbocharged SI engine. A more general and theoretical description of how these types of calculations can be done can be found in Ljung and Glad [7].

This work studies the long route EGR system further by investigating an alternative SiC-FET oxygen sensor, see Andersson et al. [1] and adding another method for estimating the mass flow in the long route EGR system when comparing different methods to estimate the EGR mass flow. The modeling in this work is sort of a continuation of the work made by Qiu [13], that focused on investigating the effects of long and short route EGR systems by assuming the gas mixture in the intake side of the engine as known. This work aims at estimating the gas mixture in the intake side of the engine and modeling the components in the long route EGR system in Simulink, to be able to simulate the gas mixture in the air intake volumes on the engine. The modeling in this work is based on measurements on a rig engine with a long route EGR system installed.

1.3 Delimitations

In this study, the lambda value is assumed to be equal to one. This means that the model in this study does not include the effects that may occur when the fuel mixture leaves lambda equal to one, for example when fuel enrichment is used to keep the exhaust temperature down. The oxygen level in the recirculated exhaust gases are also assumed to be equal to zero in this work.

When comparing the different estimation methods and the transport delay is modeled for the recirculated exhaust gases in the engine, the work is limited to static operating points for the engine, i.e. constant load and constant engine speed. This limitation was done in order to not make the thesis work too extensive.

2

System Description

2.1 Engine data

The engine in the test cell at *Vehicular systems* at *Linköping University*, on which the measurements in this thesis work was done, was a four cylinder turbocharged direct injected spark ignited engine with variable phasing of the inlet- and exhaust camshafts (iVVT and eVVT). The engine in the test cell was connected to a break so that the applied load on the engine could be controlled. The main properties of the engine is listed in Table 2.1.

Table 2.1: Geometric data for the engine

Description	Value
Number of cylinders	4 in line
Total displacement	1969cm ³
Bore	82mm
Stroke	93.2mm

The engine was equipped with several different sensors. The production sensors on the engine were connected to a modified production ECU connected to a computer, where signals could be recorded. This production ECU controlled most of the actuators on the engine, such as the throttle, iVVT and eVVT, fuel injection and so on. Parallel to the production ECU, a second ECU was used to control the long route EGR valve. The second ECU was connected to a computer where signals were recorded and control algorithms were implemented.

2.2 Silicon carbide field effect transistor oxygen sensor

One way to estimate the mass flow over the long route EGR circuit is to measure the oxygen level in the engines air intake system, see section 3.3.1 for more about the estimation method. Two oxygen sensors were installed on the engine as a part of this thesis work. One pressure compensated lambda sensor used in production and one SiC-FET prototype sensor that is developed by *FunMat* at *Linköping University*. The lambda sensor was used to collect data for the modeling and estimation in this thesis work. The SiC-FET prototype sensor was installed on the engine rig in order to test the sensor in an environment where it is intended to operate and compare the result to the data collected from the production lambda sensor. Readers interested in more technical details of the SiC-FET sensor are referred to Andersson et al. [1] and Lundström et al. [9].

The advantage of the SiC-FET sensor type compared to the lambda sensor, is that the SiC-FET sensor can operate in both cold and hot environments. The lambda sensor can not operate in environments with temperatures below 100 degrees Celsius approximately, and needs to be calibrated periodically for temperatures just above 100 degrees Celsius. The SiC-FET sensor has no degradation of the sensor output over time, and should be resistant to oil residues and be chemically inert to most substances. That would probably make the SiC-FET sensor more suited for production vehicles, if the oxygen level in the air intake would have to be measured in the engine.

During the measurements, the SiC-FET sensor measured the oxygen in the air at the same position as the lambda sensor, and the measurements from the lambda sensor were used by the sensor developers to evaluate the performance of the SiC-FET sensor. Some results from the measurements performed by the sensor developers are presented in section 4.3.

2.3 Long route EGR system

By leading cooled exhaust gases back to the intake side, advantages in emissions, fuel efficiency and performance can be achieved. Since the gases are recycled, the emissions are reduced since the gases are burned again. The pumping losses can also be reduced at low to medium load at low engine speeds since recirculated exhaust gases enable dethrottling. For high load at medium to high engine speed, the performance can be increased since the combustion temperature is reduced when cooled exhaust gases are recirculated. This decreases the risk for engine knock and enables better combustion phasing. Since the combustion temperature is decreased, the heat losses through the cylinder walls is also decreased, and fuel can be saved by leaving the fuel enrichment strategy for protecting the components on the exhaust side of the engine.

A long route EGR system recirculates the exhaust gases downstream of the tur-

bine back to the air intake side before the turbo compressor. Where the exhaust gases are taken on the exhaust side differs in the literature mentioned in section 1.2. Configurations exist where the exhaust gases are taken from the volume before the first catalyst brick, between the catalyst bricks, and after the entire catalyst. The advantage of taking the exhaust gases after the catalyst is that the gas is cleaner and contains less soot after the catalyst, but a problem that occurs is that the pressure drop over the long route EGR system decreases. If the exhaust gases are taken before the first catalyst brick, the pressure drop over the system is higher, but the gas may be dirty which can lead to clogging. Taking the gases between the two catalyst bricks in the catalyst, is a compromise of the other two options.

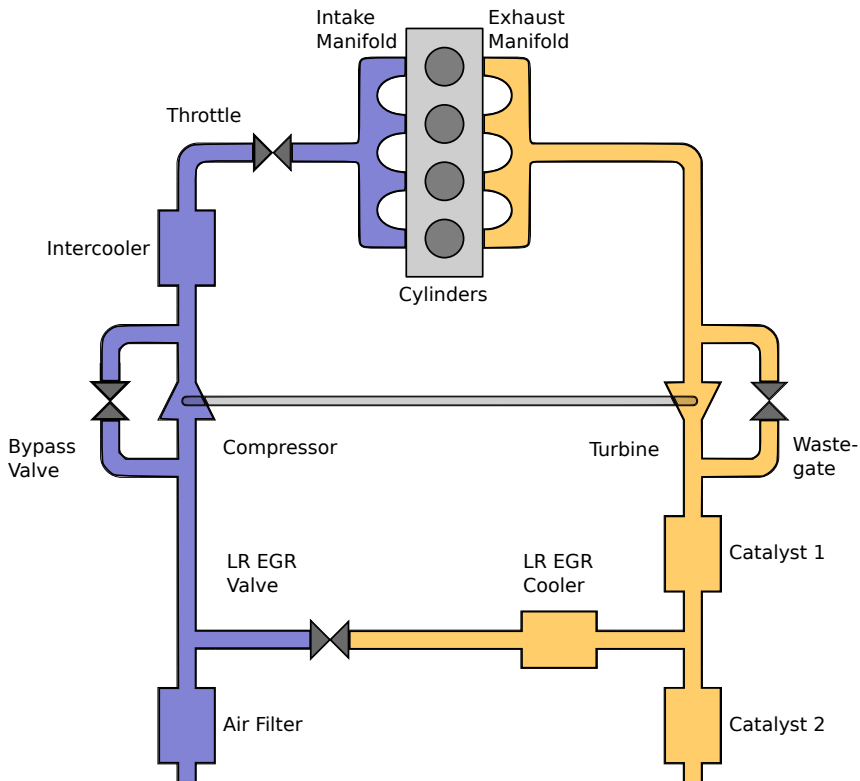


Figure 2.1: Sketch of the gas path in an engine with a long route Exhaust Gas Recirculation system. The exhaust gases after the first catalyst brick are cooled down and led back to the volume between the air filter and turbo compressor on the air intake side.

The long route EGR system that was installed on the engine rig in this work recirculates the exhaust gases from the volume after the first catalyst brick in the three way catalyst (after the turbine), to the air intake pipe before the turbo compressor. On the way, the exhaust gases are cooled down by leading the gases through a water cooled radiator. On the long route EGR system, a throttle valve controls the amount of exhaust gases that recirculates back to the intake side of the engine. Additional oxygen sensors were also installed on the pipe between the turbo compressor and the intercooler. The additional oxygen sensors were used to measure the amount of oxygen for estimating the amount of recirculated gases.

3

Long Route EGR System Modeling and Estimation Fundamentals

3.1 Modeling method

The models for the long route EGR system were implemented in an existing Simulink model for the engine type on which the measurements were done. This was done by using subsystems for the components in the long route EGR system containing models for control volumes, restrictions and heat exchange models. In order to model the gas propagation for the recirculated exhaust gases on the air intake side on the engine, a gas mixture model was included in the control volume models on the air intake side of the engine.

3.1.1 Flow restrictions

The flow restrictions can be modeled either as a laminar (3.1) or incompressible turbulent with a linear region added to the model (3.2). For higher velocities through the restriction, there is a bit more complex compressible model (3.3). One easy way to choose between those models is to fit different models for each component and see what model performs best in the validation. The following models are taken from [2]. The subscript us indicates upstream and ds indicates downstream.

The incompressible laminar restriction model is for laminar flows, which typically occurs at low flow velocities. The constant C_{la} is a design parameter in model (3.1).

Incompressible laminar restriction model:

$$\dot{m}(p_{us}, T_{us}, p_{ds}) = C_{la} \frac{p_{us}}{RT_{us}} \Delta p \quad (3.1)$$

The incompressible turbulent restriction model (3.2) with a linear region is a model for turbulent flows, but has a linear region when the pressure drop approaches zero. The reason to include a linear region is to avoid diverging derivatives in simulation environments. This model is typically suitable for pipe bends, area changes and higher flow velocities. The constant C_{tu} is a design parameter as well as the boundary for the linear region Δp_{lin} .

Incompressible turbulent restriction model with linear region:

$$\dot{m}(p_{us}, T_{us}, p_{ds}) = \begin{cases} C_{tu} \sqrt{\frac{p_{us}}{RT_{us}}} \sqrt{\Delta p}, & \text{if } p_{us} - p_{ds} \geq \Delta p_{lin} \\ C_{tu} \sqrt{\frac{p_{us}}{RT_{us}}} \frac{p_{us} - p_{ds}}{\sqrt{\Delta p_{lin}}}, & \text{otherwise} \end{cases} \quad (3.2)$$

The compressible restriction model (3.3) is suitable for components with high fluid velocity, such as throttle restrictions. For a throttle valve, the area A and the discharge coefficient C_D can be replaced with an effective area that depends on the throttle position.

Compressible restriction model:

$$\dot{m}(p_{us}, T_{us}, p_{ds}, A) = AC_D \frac{p_{us}}{\sqrt{RT_{us}}} \Psi_{li}(\Pi(\frac{p_{ds}}{p_{us}})) \quad (3.3)$$

$$\Pi(\frac{p_{ds}}{p_{us}}) = \max\left(\frac{p_{ds}}{p_{us}}, \left(\frac{2}{\gamma + 1}\right)^{\frac{\gamma}{\gamma - 1}}\right) \quad (3.4)$$

$$\Psi_0(\Pi) = \sqrt{\frac{2\gamma}{\gamma - 1} (\Pi^{2/\gamma} - \Pi^{\gamma/(\gamma - 1)})} \quad (3.5)$$

$$\Psi_{li}(\Pi) = \begin{cases} \Psi_0(\Pi), & \text{if } \Pi \leq \Pi_{li} \\ \Psi_0(\Pi_{li}) \frac{1 - \Pi}{1 - \Pi_{li}}, & \text{otherwise} \end{cases} \quad (3.6)$$

3.1.2 Control volumes

The pipes and volumes between the components in the system can be modeled as isothermal 3.7 or adiabatic 3.8 control volumes. Isothermal means that there is no heat change in the volume ($T_{in} = T_{out}$). The adiabatic model is based on the conservation of internal energy and assumes that there is no heat exchange with

the surrounding environment. When modeling the long route EGR system, the procedure for choosing volume models was the same as for the restrictions. After measurement have been done on a volume component, an isothermal model was chosen if the ingoing temperature for the mass flow was the same as the outgoing temperature. In case the outgoing temperature was different from the ingoing temperature, an adiabatic model was chosen.

Isothermal control volume model:

$$\frac{dp}{dt} = \frac{RT}{V}(\dot{m}_{in} - \dot{m}_{out}) \quad (3.7)$$

Adiabatic control volume model:

$$\begin{aligned} \frac{dT}{dt} &= \frac{1}{mc_v} \left[\dot{m}_{in}c_v(T_{in} - T) + R(T_{in}\dot{m}_{in} - T\dot{m}_{out}) - \dot{Q} \right] \\ \frac{dm}{dt} &= \dot{m}_{in} - \dot{m}_{out} \\ p &= \frac{mRT_{out}}{V} \end{aligned} \quad (3.8)$$

3.1.3 Temperature exchange

The model for describing the temperature drop in the long route EGR intercooler is described in equation (3.9). First, the heat transfer coefficient ε was assumed as constant. Then a regression model (3.10) was used to describe the heat transfer coefficient. The model with best fit compared to complexity was chosen.

Isothermal control volume model:

$$T_{ds} = T_{us} - \varepsilon(T_{us} - T_{cool}) \quad (3.9)$$

$$\varepsilon = a_0 + a_1\left(\frac{T_{cool} + T_{us}}{2}\right) + a_2\dot{m} \quad (3.10)$$

3.1.4 Gas mixture

The amount of recirculated exhaust gases on the air intake side of the engine can be described with equation (3.11).

$$X_{EGR} = \frac{m_{EGR}}{m_{tot}} = \frac{m_{EGR}}{m_{air} + m_{EGR}} \quad (3.11)$$

To simulate the amount of recirculated exhaust gases in a control volume, the model in equation (3.12) where the in- and outgoing mass flows and burned gas fractions are summed up, was used.

Differential equation model for burned gas fraction in a control volume:

$$\frac{dX_B}{dt} = \frac{RT}{pV} \sum_i (X_{B,i} - X_B) \dot{m}_i \quad (3.12)$$

Since the gas constant R is different for air compared to exhaust gases, $R_{air} = 287 \text{ J/kgK}$ and $R_{exh} = 290 \text{ J/kgK}$, the gas constant was linear interpolated with respect to the burned gas fraction X_B in the control volumes on the air intake side of the engine with equation (3.13).

$$R = R_{air} + X_B(R_{exh} - R_{air}) \quad (3.13)$$

As well as the gas constant R , the heat capacity ratio γ and the specific heat capacity at constant volume c_v and at constant pressure c_p differs between fresh air and exhaust gases. The specific heat capacity also depends non-linear on the temperature. In this study, the specific heat capacity are assumed to $c_{v,air} = 718 \text{ J/kgK}$ and $c_{v,exh} = 967 \text{ J/kgK}$. For the specific heat capacity at constant volume c_v in the control volume models, a linear interpolation with respect to the burned gas fraction X_B is made in the same way as for the gas constant R . The linear interpolation for c_v is described in equation (3.14).

$$c_v = c_{v,air} + X_B(c_{v,exh} - c_{v,air}) \quad (3.14)$$

3.2 Modeling the components of the long route EGR system

The long route EGR system was modeled in Simulink. Each component in the system was modeled with mean value engine models (MVEMs) in subsystems, to get a modular system where each model can easily be replaced. The long route EGR system was then implemented in an existing engine model in Simulink.

The parametrization of the MVEM models was done from measurements done on the engine rig. During the measurements, the engine was run at a static point in engine speed, load and position in the long route EGR valve. Then the signals that were to be recorded was measured during a few seconds so a mean value could be calculated out from the recorded data. When the static point was changed, for example in the long route EGR position, the engine was run at the new static point, typically five to ten minutes so that the temperatures of interest reached their static conditions. The data was then used to calculate the model parameters by using the least square method in Matlab.

The static operating points measured for modeling the components are listed in table 3.1. In each operating point, fourteen static points with different EGR valve positions were measured.

Table 3.1: Engine operating points during measurement when collecting data for parameterizing the MVEM models. The engine load is expressed in the unit gram air per revolution which is assumed to increase proportional to the produced torque. In each operating point, the static points for the following positions in the long route EGR valve were measured: 0, 5, 10, 15, 20, 25, 30, 35, 40, 45, 50, 60, 75 and 100 percent.

Engine speed [rpm]	Engine load [g/rev]
2500	1.7
3500	1.7
4000	1.1

3.2.1 Modeling the three-way catalyst

The three way catalyst in the Simulink engine model in which the long route EGR system was implemented, was previously modeled as one incompressible restriction with a linear region. Since the long route EGR system recirculates the exhaust gases from the volume between the first and second brick in the catalyst, a control volume model was added between the catalyst bricks and each brick was modeled with one separate restriction on each side of the control volume.

Restriction model for the first catalyst brick

The restriction models that were tested for the first catalyst brick was one laminar incompressible model (3.1) and one turbulent incompressible restriction model (3.2). The restriction model with the best fit was then implemented in Simulink. The modeled mass flow into the cylinders was used when the restriction models for the first catalyst brick were parameterized.

Model input signals: Temperature before catalyst T_{bCat} , pressure before and in catalyst p_{bCat} and p_{Cat} .

Model output signal: Mass flow through first catalyst brick \dot{m}_{cat1}

Models: Incompressible laminar restriction model:

$$\dot{m}_{cat1}(p_{bCat}, T_{bCat}, p_{cat}) = C_{la,cat1} \frac{p_{bCat}}{R_{exh} T_{bCat}} (p_{bCat} - p_{Cat}) \quad (3.15)$$

Incompressible turbulent restriction model:

$$\dot{m}_{cat1}(p_{bCat}, T_{bCat}, p_{cat}) = C_{tu,cat1} \sqrt{\frac{p_{bCat}}{R_{exh} T_{bCat}}} \sqrt{p_{bCat} - p_{Cat}} \quad (3.16)$$

Parameters to be estimated: Restriction parameter $C_{la,cat1}$ for model (3.15) and restriction parameter $C_{tu,cat1}$ for model (3.16).

Known parameters: Gas constant for exhaust gases $R_{exh} = 290 \text{ J}/(\text{kgK})$.

Control volume model between the catalyst bricks

To model the control volume between the catalyst brick, the control volume model (3.8) was used. The pressure in the volume was then determined from the ideal gas law.

Model input signals: Mass flows in and out from the volume \dot{m}_{cat1} , \dot{m}_{cat2} and \dot{m}_{EGRic} . Temperature for ingoing mass flow T_{bCat} .

Model output signal: Temperature in catalyst T_{cat} , pressure in catalyst p_{cat} .

Model:

$$\begin{cases} \frac{dT_{cat}}{dt} = \frac{1}{m_{cat} c_{v,exh}} [\dot{m}_{cat1} c_{v,exh} (T_{bCat} - T_{cat}) \\ \quad + R_{exh} (T_{bCat} \dot{m}_{cat1} - T_{cat} \dot{m}_{cat2} - T_{cat} \dot{m}_{EGRic}) - \dot{Q}] \\ \frac{dm_{cat}}{dt} = \dot{m}_{cat1} - \dot{m}_{cat2} - \dot{m}_{EGRic} \\ p_{cat} = \frac{m_{cat} R_{exh} T_{cat}}{V_{cat}} \end{cases} \quad (3.17)$$

Parameters to be estimated: None.

Known parameters: Exhaust gas constant $R_{exh} = 290 \text{ J}/(\text{kgK})$, specific heat constant at constant volume $c_{v,exh} = 997 \text{ J}/\text{kgK}$. The catalyst volume is assumed as $V_{cat} = 3 \text{ litres}$. The heat transfer \dot{Q} is assumed to be equal to zero.

Restriction model for the second catalyst brick

The restriction model for the second catalyst brick was modeled in the same way as for the first catalyst brick with one laminar incompressible model (3.1) and one turbulent incompressible restriction model (3.2). Then the model with the best fit was implemented in Simulink. The mass flow from the air filter mass flow sensor was the models were parameterized for the second catalyst brick.

Model input signals: Temperature in catalyst T_{Cat} , pressure in and after catalyst p_{Cat} and p_{es} .

Model output signal: Mass flow through second catalyst brick \dot{m}_{cat2}

Models: Incompressible laminar restriction model:

$$\dot{m}_{cat2}(p_{cat2}, T_{cat}, p_{es}) = C_{la,cat2} \frac{p_{cat}}{R_{exh} T_{cat}} (p_{cat} - p_{es}) \quad (3.18)$$

Incompressible turbulent restriction model:

$$\dot{m}_{cat2}(p_{cat2}, T_{cat}, p_{es}) = C_{tu,cat2} \sqrt{\frac{p_{cat}}{R_{exh} T_{cat}}} \sqrt{p_{cat} - p_{es}} \quad (3.19)$$

Parameters to be estimated: Restriction parameter $C_{la,cat2}$ for model (3.18) and restriction parameter $C_{tu,cat2}$ for model (3.19).

Known parameters: Gas constant for exhaust gases $R_{exh} = 290 \text{ J}/(\text{kgK})$.

3.2.2 Modeling long route EGR intercooler

The long route EGR intercooler used for this work consists of a water cooled radiator. The most significant phenomena for this component is of course the temperature exchange between the recirculated exhaust gases and the engine coolant, but the intercooler also works as a restriction and control volume.

Restriction model

The restriction model for the long route EGR intercooler was also modeled with one incompressible laminar restriction model (3.1) one incompressible turbulent restriction model with linear region (3.2). Then the restriction model with the best fit was implemented in Simulink.

Model input signals: Pressure in catalyst p_{cat} , temperature in catalyst T_{cat} and pressure between the long route EGR intercooler and the EGR valve p_{aEGRic} .

Model output signal: Mass flow through the long route EGR intercooler \dot{m}_{EGRic} .

Models: Incompressible laminar restriction model:

$$\dot{m}_{EGRic}(p_{cat}, T_{cat}, p_{aEGRic}) = C_{la,EGRic} \frac{p_{cat}}{R_{exh} T_{cat}} (p_{cat} - p_{aEGRic}) \quad (3.20)$$

Incompressible turbulent restriction model:

$$\dot{m}(p_{cat}, T_{cat}, p_{aEGRic}) = C_{tu,EGRic} \sqrt{\frac{p_{cat}}{R_{exh} T_{cat}}} \sqrt{(p_{cat} - p_{aEGRic})} \quad (3.21)$$

Parameters to be estimated: Restriction parameter $C_{la,EGRic}$ for model (3.20) and restriction parameter $C_{tu,EGRic}$ for model (3.21).

Known parameters: Gas constant for exhaust gases $R_{exh} = 290 \text{ J}/(\text{kgK})$.

Temperature cooling model

The model used to describe the temperature drop from the catalyst to after the long route EGR intercooler is described in (3.22). The coolant temperature T_{cool} was assumed as constant and was set to the mean value of the observed temperatures during the measurements. One model with constant heat transfer coefficient ε was estimated and one model with a regression model for the heat transfer coefficient ε was created. If the model with a constant efficiency constant ε would result in a bad model fit, model (3.23) would be used to describe the efficiency coefficient instead.

Model input signals: Temperature in catalyst T_{cat} , mass flow through long route EGR intercooler \dot{m}_{EGRic} .

Model output signal: Temperature after the long route EGR intercooler T_{aEGRic} .

Model:

$$T_{aEGRic} = T_{cat} - \varepsilon(T_{cat} - T_{cool}) \quad (3.22)$$

$$\varepsilon = a_0 + a_1 \left(\frac{T_{cool} + T_{cat}}{2} \right) + a_2 \dot{m}_{EGR} \quad (3.23)$$

Parameters to be estimated: Long route intercooler efficiency coefficient ε for the model with constant coefficient, and parameter a_0 , a_1 and a_2 for the regression model.

Known parameters: The engine coolant temperature assumed as constant to $T_{cool} = 100$ degrees Celsius.

Control volume model

A control volume was added between the long route EGR intercooler and the long route EGR valve to be able to connect the restriction models in Simulink. The model that was used was the adiabatic control volume model with temperature and mass as states (3.8). The long route intercooler volume was assumed as $V_{EGRic} = 1$ lite in this model. The variable m_{EGRcv} represents the mass state in the control volume.

Model input signals: Temperature after the long route EGR intercooler T_{aEGRic} , mass flow in and out from the control volume \dot{m}_{EGRic} and \dot{m}_{EGRvlv}

Model output signal: Temperature before the long route EGR valve $T_{bEGRvlv}$ and pressure after the long route EGR intercooler p_{EGRic} .

Model:

$$\begin{cases} \frac{dT_{bEGRvlv}}{dt} &= \frac{1}{m_{EGRcv}c_{v,exh}} [\dot{m}_{EGR}c_{v,exh}(T_{aEGRic} - T_{bEGRvlv}) \\ &+ R_{exh}(T_{aEGRic}\dot{m}_{EGRic} - T_{bEGRvlv}\dot{m}_{EGRvlv}) - \dot{Q}] \\ \frac{dm_{EGRcv}}{dt} &= \dot{m}_{EGRic} - \dot{m}_{EGRvlv} \\ p_{EGRic} &= \frac{m_{EGRcv}R_{exh}T_{bEGRvlv}}{V_{EGRic}} \end{cases} \quad (3.24)$$

Parameters to be estimated: None.

Known parameters: Exhaust gas constant $R_{exh} = 290 \text{ J/(kgK)}$, specific heat constant at constant volume $c_{v,exh} = 997 \text{ J/kgK}$. The control volume in the long route EGR intercooler was assumed as $V_{EGRic} = 1 \text{ litre}$. The heat transfer \dot{Q} is assumed to be equal to zero.

3.2.3 Modeling the long route EGR valve

The valve that controlled the mass flow through the long route EGR system was a throttle valve. The valve was modeled as a compressible turbulent restriction, model equations (3.3) to (3.6). The area A and the discharge coefficient C_D in (3.3) was replaced with an effective area A_{eff} that depends on the valve position u . The valve position for the valve was normalized so that $u_{EGR} = 0$ represents a closed valve and $u_{eff} = 1$ represents a fully open valve. The effective area in this work was provided by the engine manufacturer.

The compressible turbulent restriction model used here also includes a linear region in order to satisfy the Lipschitz condition and avoid oscillations in simulations at pressure drops close to zero. The parameter for the linear region was set to $\Pi_{lin} = 0.9$.

Model input signals: $p_{bef,comp}$, $p_{aft,EGRic}$

Model output signal: \dot{m}_{EGR}

Model: Compressible restriction model (3.3):

$$\dot{m}_{EGR}(p_{us}, T_{us}, p_{ds}, A_{eff}) = A_{eff} \frac{p_{aEGRic}}{\sqrt{RT_{aEGRic}}} \Psi_{li}(\Pi) \left(\frac{p_{bComp}}{p_{aEGRic}} \right) \quad (3.25)$$

$$\Pi \left(\frac{p_{bComp}}{p_{aEGRic}} \right) = \max \left(\frac{p_{bComp}}{p_{aEGRic}}, \left(\frac{2}{\gamma_{exh} + 1} \right)^{\frac{\gamma_{exh}}{\gamma_{exh} - 1}} \right) \quad (3.26)$$

$$\Psi_0(\Pi) = \sqrt{\frac{2\gamma_{exh}}{\gamma_{exh} - 1} (\Pi^{2/\gamma_{exh}} - \Pi^{\gamma_{exh}/(\gamma_{exh} - 1)})} \quad (3.27)$$

$$\Psi_{li}(\Pi) = \begin{cases} \Psi_0(\Pi), & \text{if } \Pi \leq \Pi_{li} \\ \Psi_0(\Pi_{li}) \frac{1 - \Pi}{1 - \Pi_{li}}, & \text{otherwise} \end{cases} \quad (3.28)$$

Parameters to be estimated: Linear region Π_{lin} for restriction model if the suggested value $\Pi_{lin} = 0.9$ would cause oscillations during simulation.

Known parameters: Heat capacity ratio for exhaust gases γ_{exh} , effective area for the EGR valve A_{eff} .

The obtained effective area for the valve used in this work consisted of several data points for the effective area at certain valve positions. When the restriction model for the long route EGR was implemented in Simulink, a look-up table was used to interpolate the effective area with respect to the EGR valve position.

3.2.4 Gas mixture in air intake control volumes

The gas mixture model for each control volume was derived from equation (3.12) and implemented in the existing control volumes in the Simulink model.

Air filter control volume

Model (3.29) was implemented in the control volume between the air filter model and compressor model in Simulink to describe the burned gas fraction.

$$\frac{dX_B}{dt} = \frac{RT}{pV} [X_{B,air} \dot{m}_{AF} + X_{B,EGR} \dot{m}_{EGR} + X_{B,Comp,cv} \dot{m}_{BPvlv} - X_B \dot{m}_{Comp} - X_B (\dot{m}_{AF} + \dot{m}_{EGR} + \dot{m}_{BPvlv} - \dot{m}_{Comp})] \quad (3.29)$$

Compressor control volume

Model (3.30) was implemented in the control volume between the compressor model and intercooler model in Simulink to describe the burned gas fraction.

$$\frac{dX_B}{dt} = \frac{RT}{pV} [X_{B,AFcv} \dot{m}_{Comp} - X_{B,CompCV} \dot{m}_{BPvlv} - X_{B,CompCV} \dot{m}_{IC} - X_B (\dot{m}_{Comp} - \dot{m}_{BPvlv} - \dot{m}_{IC})] \quad (3.30)$$

Intercooler control volume

Model (3.31) was implemented in the control volume between the intercooler model and throttle model in Simulink to describe the burned gas fraction.

$$\frac{dX_B}{dt} = \frac{RT}{pV} [X_{B,CompCV} \dot{m}_{IC} - X_{B,ICcv} \dot{m}_{thr} - X_B (\dot{m}_{IC} - \dot{m}_{thr})] \quad (3.31)$$

Intake manifold control volume

Model (3.32) was implemented in the control volume between the throttle model and the engine block model in Simulink to describe the burned gas fraction.

$$\frac{dX_B}{dt} = \frac{RT}{pV} [X_{B,ICcv} \dot{m}_{thr} - X_{B,im} \dot{m}_{cyl} - X_B (\dot{m}_{thr} - \dot{m}_{cyl})] \quad (3.32)$$

3.3 Estimating mass flow in the long route EGR system

On the engine used in this study, the air mass flow is measured before the point where the recirculated gases from the long route EGR are mixed with the fresh air, see Figure 2.1. Since the mass flow over the long route EGR system is not measured, it has to be estimated for parametrization and validation of the models. One method to estimate the long route EGR mass flow, is to use the air mass flow sensor located between the air filter and the mixing point, and measure the amount of oxygen after the mixing point. The mass flow over the long route EGR system can also be estimated by measuring the pressure difference over the long route EGR valve and the temperature before the valve. Then the mass flow can be calculated from the throttle restriction model. If the mass flow in to the cylinders can be measured or accurately estimated from a model, another method is to subtract measured fresh air mass flow from the cylinder mass flow at static conditions.

3.3.1 Estimating mass flow by measuring the oxygen

The amount of oxygen in a gas X_O can be described by Equation (3.33).

$$X_O = \frac{m_O}{m_{tot}} \quad (3.33)$$

In the air intake pipe where the air and the recirculated exhaust gases are mixed, the amount of oxygen in the mixed gas can be described by Equation (3.34).

$$X_O = \frac{X_{O,air} m_{air} + X_{O,EGR} m_{EGR}}{m_{air} + m_{EGR}} \quad (3.34)$$

To obtain the mass flow through the long route EGR valve at stationary operating points, the masses m_{air} and m_{EGR} in Equation (3.34) can be replaced with the corresponding mass flows \dot{m}_{air} and \dot{m}_{EGR} . By solving that equation for \dot{m}_{EGR} , equation (3.35) is obtained.

$$\dot{m}_{EGR} = \dot{m}_{air} \frac{X_{O,air} - X_O}{X_O - X_{O,EGR}} \quad (3.35)$$

3.3.2 Estimating mass flow by measuring the pressure difference over the long route EGR valve

By using the restriction model for the long route EGR valve, equations (3.25) to (3.28), the mass flow was determined from the pressure before and after the valve (p_{aEGRic} and p_{af}) as well as the temperature before the valve T_{aEGRic} . The current effective area A_{eff} in the valve was interpolated from the given data set that describes how the effective area in the valve depends on the valve position u_{EGRvlv} that was measured on the valve that was mounted on the engine rig.

3.3.3 Estimating mass flow from the volumetric efficiency model

If the mass flow into the cylinders is known from measurements or accurate estimation, the long route EGR mass flow can be estimated if the fresh air mass flow is measured between the air filter and the mixing point.

On the the engine in this study, the mass flow into the cylinders is estimated in the ECU. This signal can be used to calculate the mass flow over the long route EGR circuit from the simple relation in equation (3.36), where \dot{m}_{air} refers to the fresh air mass flow measured before the mixing point.

$$\dot{m}_{EGR} = \dot{m}_{cyl} - \dot{m}_{air} \quad (3.36)$$

3.4 Estimating and modeling transport delays for recirculated gases

When the Long Route EGR valve is opened and exhaust gases start to flow through the valve into the air intake pipe after the air filter, it takes some time until the recirculated exhaust gases reach the intake manifold and enter the cylinders. In this chapter, the time delays from the long route EGR valve to the cylinders are modeled. Figure 3.1 shows a sketch of the air intake side and the sections that are mentioned later in this section.

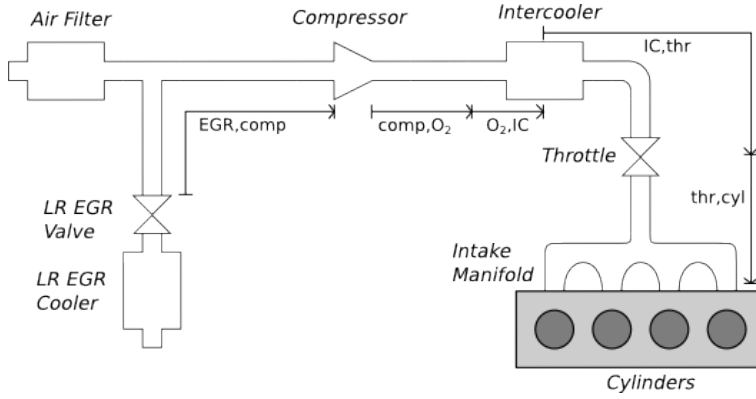


Figure 3.1: Sketch of the air intake side of the engine. The arrows next to the pipes indicates the sections for which the time delays were modeled.

The expression for describing the time delay τ was derived from the relation between time, velocity and distance:

$$\tau = \frac{L}{v} \quad (3.37)$$

The velocity for a fluid in a pipe can be described by equation (3.38) where \dot{V} represents the volume flow and A the cross sectional area of the pipe.

$$v = \frac{\dot{V}}{A} \quad (3.38)$$

The volume flow can be expressed as mass flow \dot{m} divided by the density of the fluid ρ :

$$\dot{V} = \frac{\dot{m}}{\rho} \quad (3.39)$$

The density of the fluid can be obtained by rewriting the ideal gas law:

$$pV = mRT \Leftrightarrow \rho = \frac{m}{V} = \frac{p}{RT} \quad (3.40)$$

From these expressions, the fluid velocity can be described by equation (3.41).

$$v = \frac{\dot{m}RT}{pA} \quad (3.41)$$

To get the expression the expression for the transport delay for a fluid in a pipe section, equation (3.41) that describes the fluid velocity was inserted into equation (3.37):

$$\tau = \frac{pAL}{\dot{m}RT} \quad (3.42)$$

Since the cross-section area for the pipe on the engine is quite irregular and varies along the pipe, the pipe area A and pipe length L were replaced with a constant C_{pipe} that works as a model design parameter. By doing so, the pipe characteristics C_{pipe} can be estimated from measurements on a rig engine. This may in many cases be easier than determining those parameters manually if the pipe has an irregular design with many bends and varying cross section area.

$$\tau = \frac{p}{\dot{m}RT} C_{pipe} \quad (3.43)$$

Since the prevailing conditions are different along the way from the long route EGR valve to the cylinders, the transport delay from one point to another was described by adding one time delay model described by equation (3.43) for each section. For example, when the transport delay from the long route EGR valve to the oxygen sensor located on the pipe between the turbo compressor and intercooler was modeled, one term was used to describe the time delay from the long route EGR valve to the turbo compressor and one term was used to describe the time delay for the last section from the turbo compressor to the oxygen sensor, see equation (3.44). The reason for using two terms was that the temperature and pressure increases significantly after the turbo compressor if the engine runs at a point with high boost pressure.

$$\tau_{EGRvlv,O_2} = \frac{P_{bComp}}{\dot{m}RT_{bComp}} C_{EGRvlv,comp} + \frac{P_{bIC}}{\dot{m}RT_{bIC}} C_{comp,O_2} \quad (3.44)$$

In the same way, the transport delay between the oxygen sensor and the cylinders was modeled with separate terms for each section. Here one term was used to describe the section from the oxygen sensor to the intercooler. Then one term was used to describe the section after the intercooler to the throttle. The reason to use separate terms before and after the intercooler was because the temperature drop over the intercooler leads to higher density, which at constant mass flow means that the volume flow decreases and the velocity in the pipe decreases. One last term was added to describe the time delay for the last section from the throttle to the cylinders. The obtained model for the transport delay of the fluid from the oxygen sensor to the cylinders is described in equation (3.45).

$$\tau_{O_2,cyl} = \frac{P_{bIC}}{\dot{m}RT_{bIC}} C_{O_2,IC} + \frac{P_{aIC}}{\dot{m}RT_{aIC}} C_{IC,thr} + \frac{P_{im}}{\dot{m}RT_{im}} C_{thr,cyl} \quad (3.45)$$

Finally, one model for describing the transport delay all the way from the long route EGR valve to the cylinders was set up in the same way as for the previous models, see equation (3.46).

$$\begin{aligned} \tau_{EGRvlv,O_2} = & \frac{p_{bComp}}{\dot{m}RT_{bComp}} C_{EGRvlv,comp} + \frac{p_{bIC}}{\dot{m}RT_{bIC}} C_{comp,IC} \\ & + \frac{p_{aIC}}{\dot{m}RT_{aIC}} C_{IC,thr} + \frac{p_{im}}{\dot{m}RT_{im}} C_{thr,cyl} \end{aligned} \quad (3.46)$$

The design parameters in the models (3.44), (3.45) and (3.46) were parametrized by using data collected from measurements on the engine rig. The measurements were done by running the engine at static points for different loads and engine speeds. Then a step was made in the long route EGR valve position from 0% to 50%. The signals measured during these measurements are presented in Table 3.2 and the measured operating points in Table 3.3.

Table 3.2: Signals measured during measurements when collecting data for parameterizing the transport delay models for the fluids in the air intake pipes of the engine.

Signal	Description
EGR_{pos}	Long route EGR valve position
\dot{m}	Mass flow through air filter
p_{bComp}	Pressure before compressor
T_{bComp}	Temperature before compressor
p_{bIC}	Pressure before intercooler
T_{bIC}	Temperature before intercooler
O_2	Oxygen level between turbo compressor and intercooler
p_{aIC}	Pressure after intercooler
T_{aIC}	Temperature after intercooler
p_{im}	Pressure in intake manifold
T_{im}	Temperature in intake manifold
p_{cy1}	Pressure in cylinder number one
p_{cy2}	Pressure in cylinder number two
p_{cy3}	Pressure in cylinder number three
p_{cy4}	Pressure in cylinder number four

Table 3.3: Engine operating points used during the measurements when collecting data for parameterizing the transport delay models for the fluids in the air intake pipes of the engine. The engine load is expressed in the unit gram air per revolution, which is assumed to increase proportional to the produced torque.

#	Engine speed [rpm]	Engine load [g/rev]
1	1500	0.7
2	1500	1
3	1750	0.7
4	1750	1
5	2000	0.7
6	2000	1
7	2250	0.7
8	2250	1
9	2500	1
10	2500	1.3
11	2500	1.5
12	3000	1
13	3000	1.3
14	3000	1.5
15	3000	1.7
16	3500	1.1
17	3500	1.3
18	3500	1.5
19	3500	1.7
20	4000	1.1
21	4000	1.3
22	4000	1.5
23	4000	1.7

The time from when the EGR valve position started to change to when the oxygen level started to change was used to calculate the transport time τ_{EGRvlv, O_2} for each operating point. The time from the first change in oxygen level to the first detected change in the cylinder pressure was then used to calculate the transport time $\tau_{O_2, cyl}$ from the oxygen sensor to the cylinders. The time when the EGR valve started to change position t_{EGRvlv} was determined out from the recorded position signal for the valve. Figure 3.2 shows a plot of the measured data for the EGR valve position, the sample time for the EGR valve position signal was 100 Hz.

The time when the oxygen level started to change, t_{O_2} , was read out in the same way as for the EGR valve position. Figure 3.3 shows a plot of the oxygen level from the lambda sensor. The sample time for the oxygen level signal was 100 Hz.

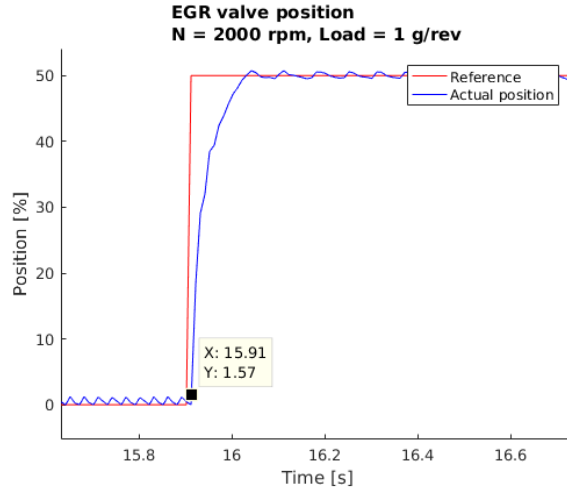


Figure 3.2: Measured data of the EGR valve position when a step was made from 0% to 50%. The data point indicates at what phase in the step the times for the EGR valve opening are measured, in this case at $t_{EGR,vlv} = 15.91$ seconds.

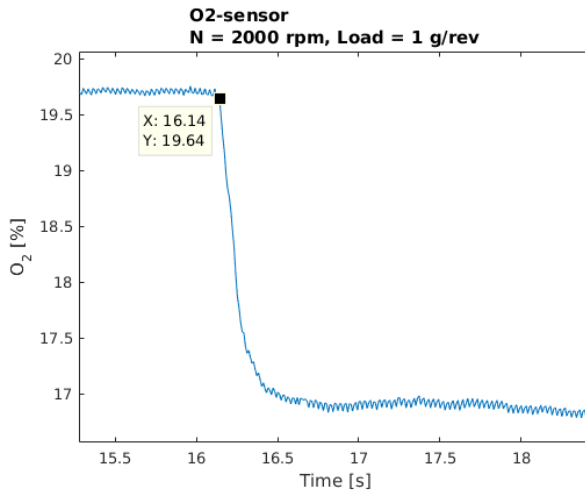


Figure 3.3: Measured data of the oxygen level between the turbo compressor and intercooler after a step has been made from 0% to 50% in the EGR valve. The data point shows when the time was measured, in this case at $t_{O_2} = 16.14$ seconds.

Figure 3.4 shows a plot of the measured cylinder pressure, which changes when the recirculated exhaust gases enters the cylinders. The time when the exhaust

gases entered the cylinders t_{cyl} was read out from the plot as soon as the change in cylinder pressure was detected.

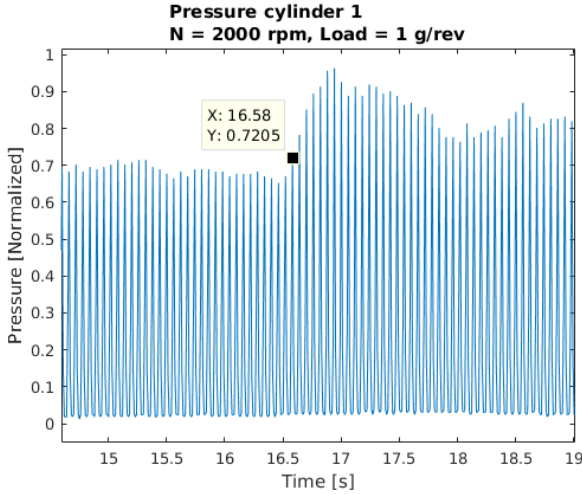


Figure 3.4: Measured data of the pressure in cylinder one of four after a step has been made from 0% to 50% in the EGR valve. The data point indicates where the exhaust gases were assumed to have entered the cylinders, in this case at $t_{cyl1} = 16.58$ seconds.

Since the cylinder pressure was measured in all of the four cylinders, an average time was calculated for when the exhaust gases entered the cylinders according from (3.47) to get a more accurate value.

$$t_{cyl} = \sum_{i=1}^{n_{cyl}} \frac{t_{cyl,i}}{n_{cyl}} \quad (3.47)$$

The time delays from the measurements was then calculated according to equation (3.49), (3.50) and (3.51).

$$\tau_{EGRvlv,O_2} = t_{O_2} - t_{EGR,vlv} \quad (3.48)$$

$$\tau_{O_2,cyl} = t_{cyl} - t_{O_2} \quad (3.49)$$

$$\tau_{EGRvlv,cyl} = t_{cyl} - t_{EGR,vlv} \quad (3.50)$$

$$(3.51)$$

After the time constants had been measured, the model parameters in equation (3.44), (3.45) and (3.46) were estimated with the least square method. The pres-

sure and temperature that were used were calculated mean values at each static operating point before the step was made in the long route EGR throttle.

The model for the time delay was then implemented to the engine model in Simulink by using the simulated values for pressure, temperature and mass flows. Then a variable transport delay block was added to the burned gas fraction signal before the control volumes that corresponds to the the control volumes to which the time delays were modeled. Figure 3.5 shows the transport delay model and the time delay block between the control volume before and after the compressor.

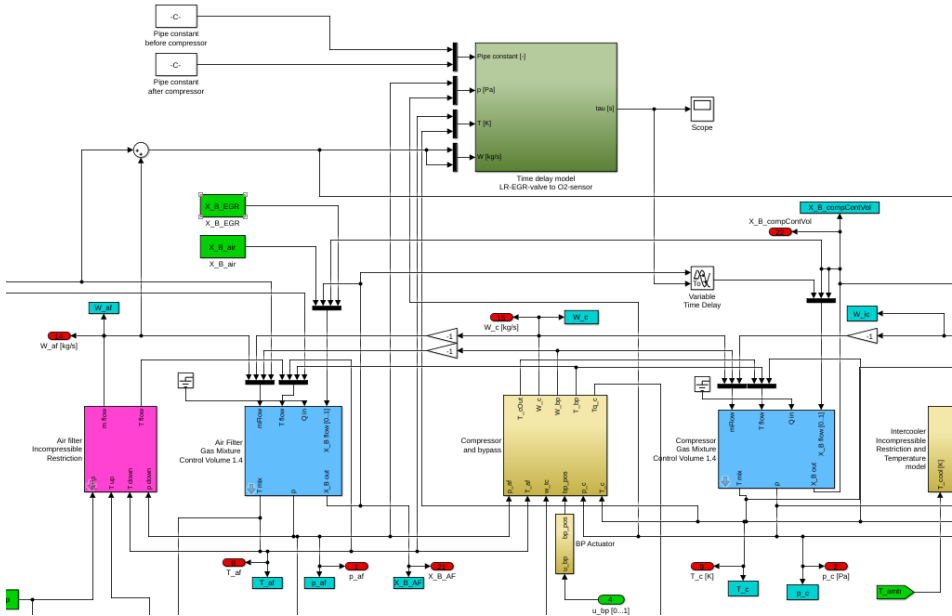


Figure 3.5: A snapshot of the time delay model in the Simulink engine model. The dark green box contains model (3.44). The blue box to the left contains the control volume between the air filter and the compressor, and the blue box to the right contains the control volume between the compressor and intercooler. The block containing the transport delay model has been built so that the same block can be used for different places. The signals and the pipe parameter constants for the modeled pipe sections are multiplexed before the subsystem.

4

Results

The performance of the created models was measured by comparing the modeled result with the measured result. This was done by plotting the modeled values against the measured values, and by calculating the mean absolute error Δx and the mean relative error δ_x . The absolute error was calculated as in equation (4.1) and the relative error as in equation (4.2), where x represents the "true" value, in this case the measured value, and x_0 represents the modeled value.

$$\Delta x = x - x_{calc} \quad (4.1)$$

$$\delta_x = \frac{x - x_{calc}}{x} \quad (4.2)$$

The mean absolute error for a series of data was calculated with equation (4.3).

$$\Delta \bar{x} = \frac{|\Delta x_1| + |\Delta x_2| + \dots + |\Delta x_n|}{n} \quad (4.3)$$

The mean relative error for a series of data was calculated with equation (4.4).

$$\bar{\delta}_x = \frac{|\delta_{x,1}| + |\delta_{x,2}| + \dots + |\delta_{x,n}|}{n} \quad (4.4)$$

4.1 Model validation

After the MVEM models had been parametrised by using the least square method in Matlab, the models were validated by plotting the modeled values against the measured values.

4.1.1 Catalyst

The validation for the mass flow through the first catalyst brick is presented in Figure 4.1 and 4.2, where Figure 4.1 represents the linear model and Figure 4.2 represents the turbulent model with a linear region. The mass flow that was used for modeling and validation of the first catalyst brick was the mass flow through the cylinders \dot{m}_{cyl} , that was provided from the ECU.

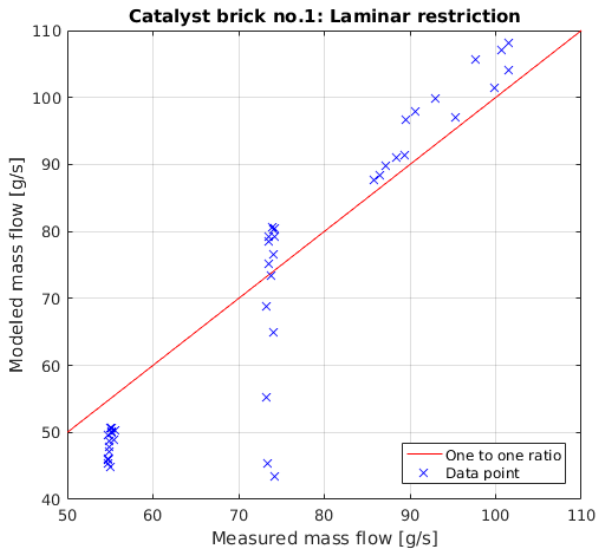


Figure 4.1: Measured mass flow compared to the modeled mass flow through the first catalyst brick using a laminar incompressible restriction model.

The turbulent model with a linear region was assessed as the most accurate model and was therefore implemented in the Simulink model.

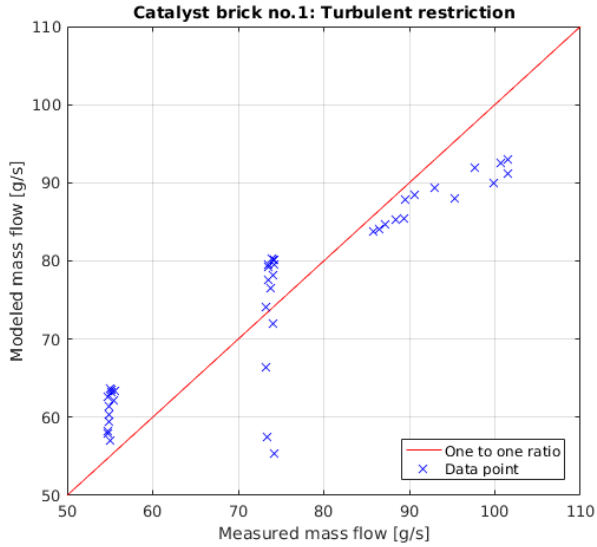


Figure 4.2: Measured mass flow compared to the modeled mass flow through the first catalyst brick using a turbulent incompressible restriction model with a linear region with $\Delta p_{lin} = 4$ kPa.

The validation for the mass flow through the second catalyst brick is presented in Figure 4.3 and 4.4, where Figure 4.3 represents the linear model and Figure 4.4 represents the turbulent model with a linear region. The mass flow that was used for modeling and validation of the second catalyst brick was the measured mass flow through the air filter \dot{m}_{air} .

The turbulent model with a linear region was assessed as the most accurate model and was therefore implemented in the Simulink model.

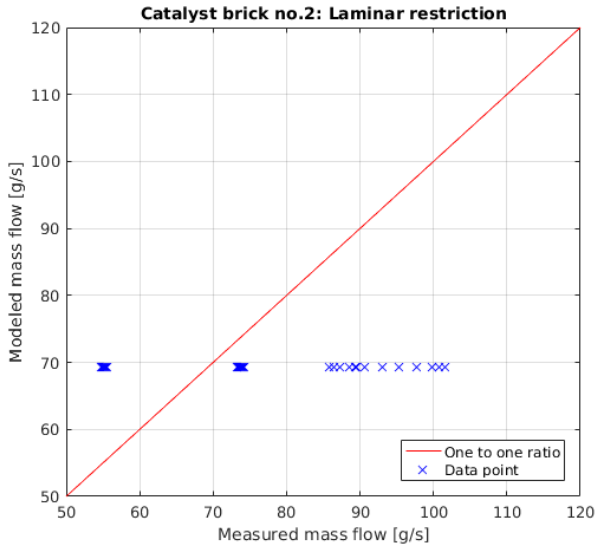


Figure 4.3: Measured mass flow compared to the modeled mass flow through the second catalyst brick using a laminar incompressible restriction model.

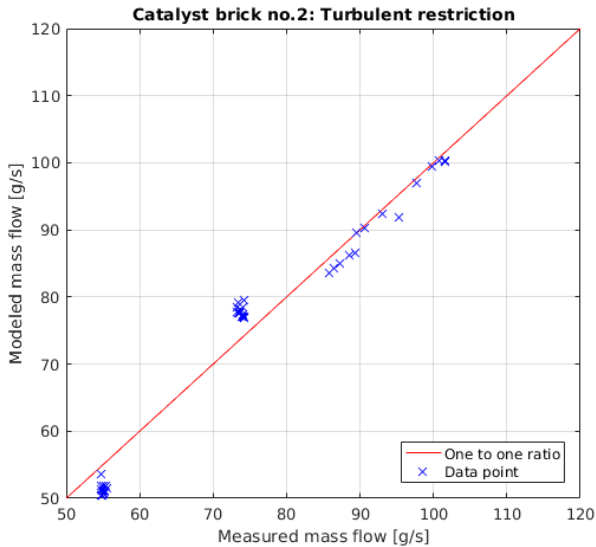


Figure 4.4: Measured mass flow compared to the modeled mass flow through the second catalyst brick using a turbulent incompressible restriction model with a linear region with $\Delta p_{lin} = 3 \text{ kPa}$.

4.1.2 Long route EGR intercooler

The validation of the restriction models for the long route EGR intercooler is presented in Figures 4.5 and 4.6, where Figure 4.5 shows the linear model and Figure 4.6 shows the turbulent model with a linear region. The mass flow that was used when modeling these models was the mass flow estimated from the oxygen sensor and air mass flow sensor.

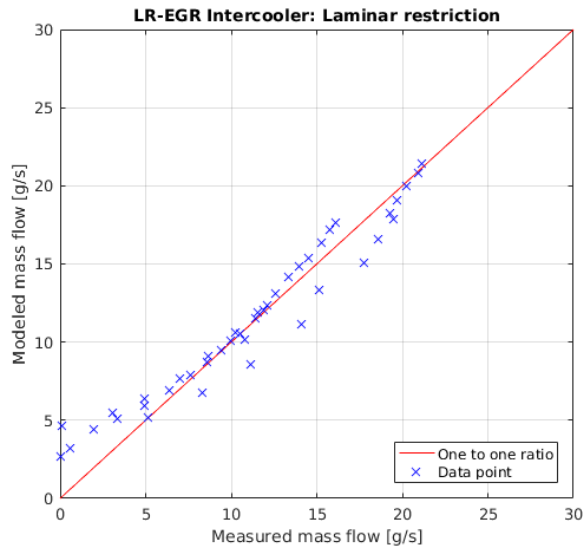


Figure 4.5: Estimated mass flow compared to the modeled mass flow through the long route EGR intercooler using a laminar incompressible restriction.

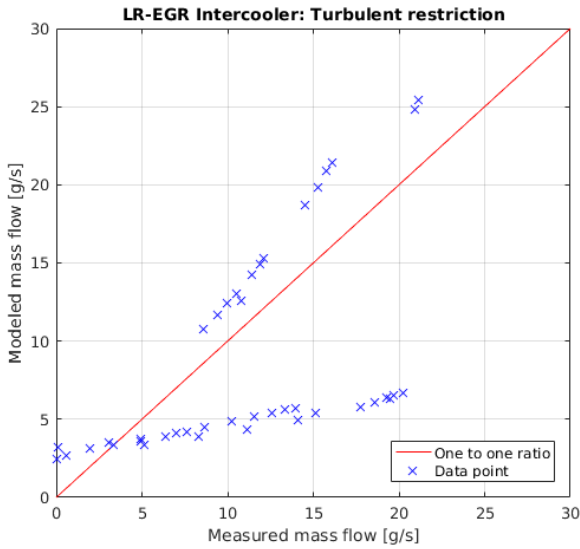


Figure 4.6: Estimated mass flow compared to the modeled mass flow through the long route EGR intercooler using a turbulent incompressible restriction model with a linear region with $\Delta p_{lin} = 600 \text{ Pa}$.

The laminar model was assessed as the most accurate model and was therefore implemented in the Simulink model.

Temperature model

The validation of the temperature model described in section 3.2.2 is presented in Figure 4.7. The result shows that the model with a non-constant heat transfer coefficient ε resulted in a better fit. The temperature model with the modeled heat transfer coefficient was therefore implemented in the Simulink model.

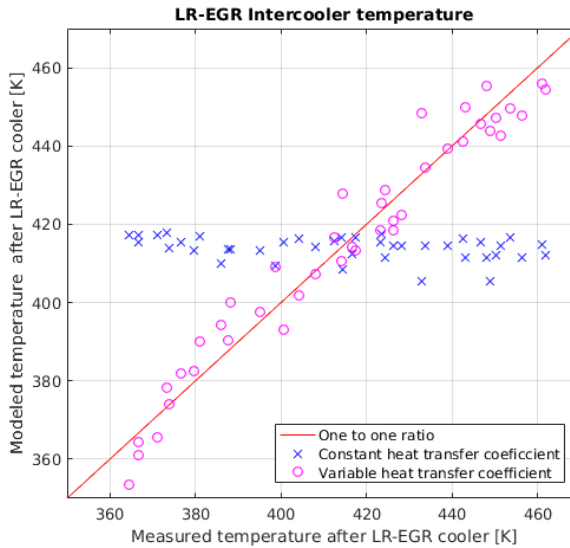


Figure 4.7: Measured temperature compared with the modeled temperature between the long route EGR intercooler and the long route throttle.

4.1.3 Long route EGR valve

The validation of the EGR valve restriction model (3.25) to (3.28) is presented in figure 4.8. The mass flow that was used when modeling this model was the mass flow calculated from the modeled mass flow into the cylinders and the measured mass flow trough the air filter, described in equation (3.36).

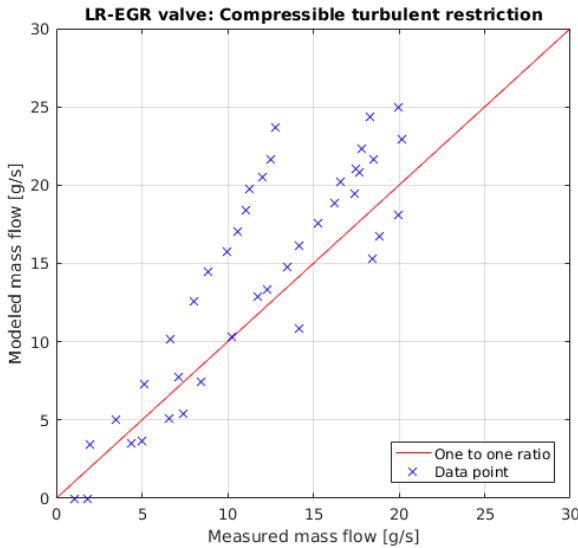


Figure 4.8: Estimated mass flow compared to the modeled mass flow trough the long route EGR valve using a turbulent compressible restriction model with $\Pi_{lin} = 1$.

4.2 Estimation of long route EGR mass flow

Figure 4.9 shows the burned gas fraction estimated from the three different methods of estimating the mass flow. The result shows that estimating the mass flow from the modeled cylinder mass flow gives similar result as when estimating the mass flow by measuring the oxygen level. Measuring the mass flow from the pressure difference over the EGR valve by using the restriction model for the valve, generally resulted in a lower value than for the two other methods.

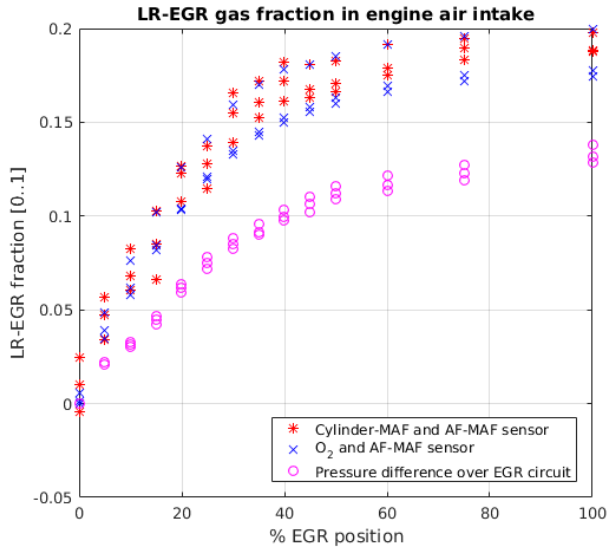


Figure 4.9: Calculated gas fraction for three different estimation methods. The method where the burned gas fraction is estimated from modeled cylinder mass flow and MAF-sensor gives similar results as the method when the burned gas fraction is estimated from the oxygen sensor and the MAF-sensor. Estimating the burned gas fraction from the pressure difference over the long route EGR valve generally resulted in a lower value than the other two methods.

4.3 Measurement with the SiC-FET oxygen sensor

The measurement with the SiC-FET sensor preformed by the sensor developers at *FunMat, Linköping University* is presented in figure 4.10. A zoomed in plot of figure 4.10 is presented in figure 4.11.

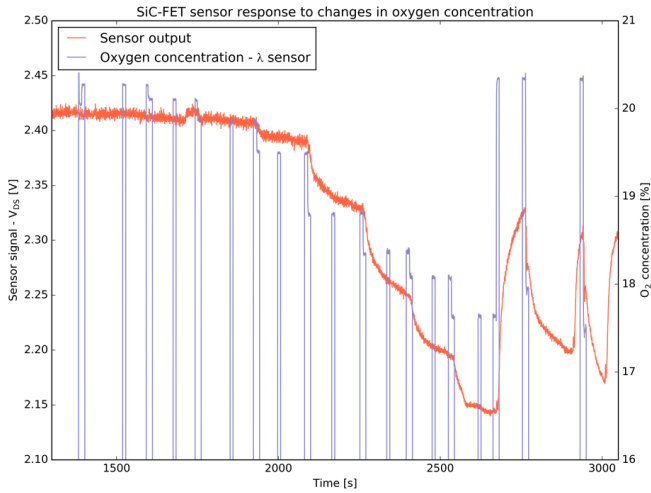


Figure 4.10: Sensor output from the measurements with the SiC-FET oxygen sensor. The red line represents the sensor output from the SiC-FET sensor, and the blue line represents the sensor output from the lambda sensor. The output from the lambda sensor was only recorded under shorter sequences, which explains the "steps" for the blue line of the plot.

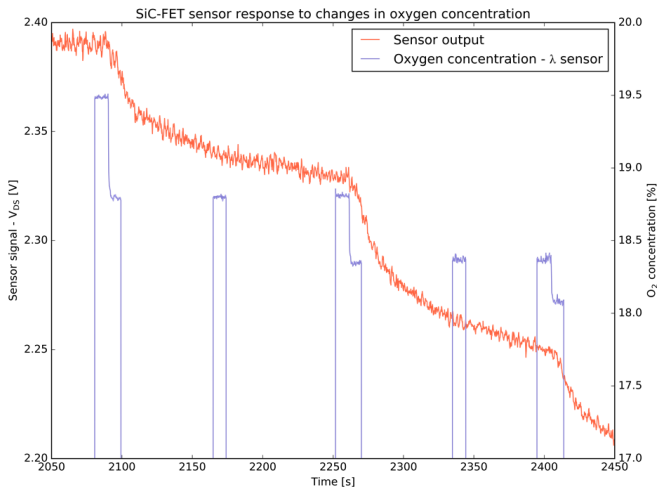


Figure 4.11: A zoom in of the plot in figure 4.10.

4.4 Estimating and modeling transport delays for recirculated gases

4.4.1 Time estimation models

The models for the transport time for gases in the intake side of the engine was validated in the same way as the MVEM models. The modeled time was plotted against the observed times from the measurements.

The validation of model (3.44) is presented in figure 4.12. The mean absolute error $\Delta \bar{t}_{EGRvlv,O_2}$ for the data points in figure 4.12 is $\Delta \bar{t}_{EGRvlv,O_2} = 0.01$ seconds, and the mean relative error $\bar{\delta}_{t_{EGRvlv,O_2}} = 5.6\%$.

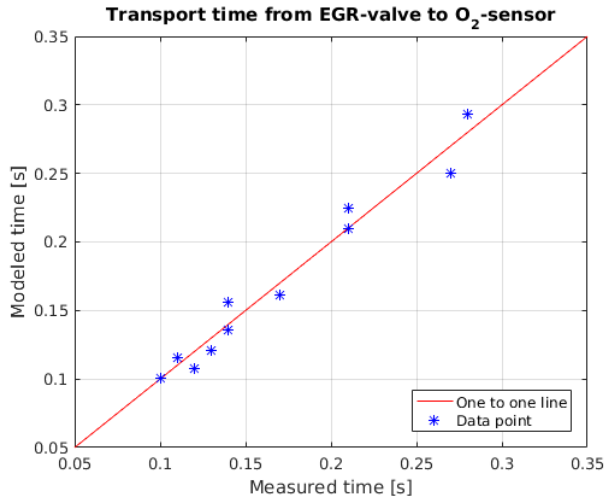


Figure 4.12: Validation of model (3.44) that describes the transport time for recirculated gases between the long route EGR valve and the oxygen sensor. The transport times for data points 2,4,...,22 in Table 3.3 were used for validation of the model, while data points 1,3,...,23 were used for modeling.

The validation for model (3.45) is presented in figure 4.13. The mean absolute error $\Delta \bar{t}_{O_2,cyl}$ for the data points in figure 4.13 is $\Delta \bar{t}_{O_2,cyl} = 0.07$ seconds, and the mean relative error $\bar{\delta}_{t_{O_2,cyl}} = 19.4\%$.

The validation for model (3.46) is presented in figure 4.14. The mean absolute error $\Delta \bar{t}_{EGRvlv,cyl}$ for the data points in figure 4.14 is $\Delta \bar{t}_{EGRvlv,cyl} = 0.08$ seconds, and the mean relative error $\bar{\delta}_{t_{EGRvlv,cyl}} = 13.5\%$.

Since the mean absolute error $\Delta t_{EGRvlv,cyl}$ for model (3.46) that describes the transport time for recirculated gases between the long route EGR valve and the cylinders was equal to the combined relative errors for the other two models

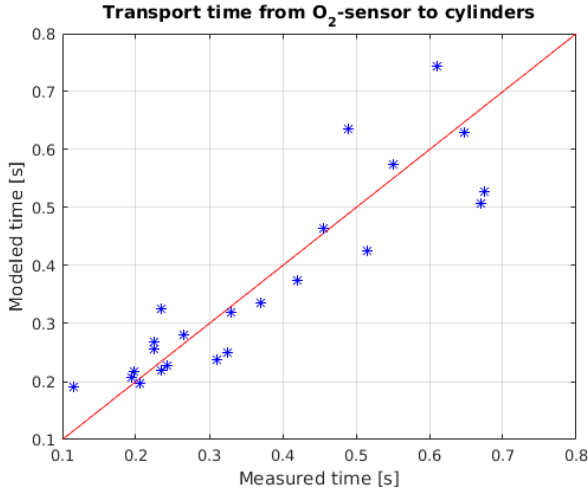


Figure 4.13: Validation of model (3.45) that describes the transport time for recirculated gases between the the oxygen sensor and the cylinders. The transport times for data points 2,4,...,22 in Table 3.3 were used for validation of the model, while data points 1,3,...,23 were used for modeling.

(3.44) and (3.45), i.e. $\Delta \bar{t}_{EGRvlv,O_2} + \Delta \bar{t}_{O_2,cyl} = \Delta \bar{t}_{EGRvlv,cyl}$, the model (3.44) and (3.45) were implemented in the Simulink model.

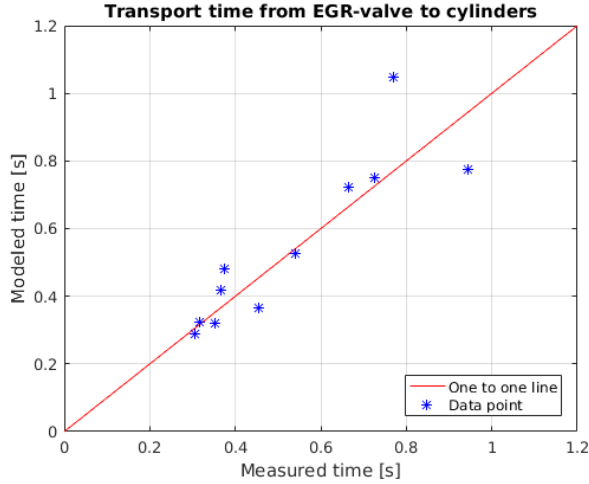


Figure 4.14: Validation of model (3.46) that describes the transport time for recirculated gases between the long route EGR valve and the cylinders. The transport times for data points 2,4,...,22 in Table 3.3 were used for validation of the model, while data points 1,3,...,23 were used for modeling.

A certain absolute error in the time estimation may have different dignity depending on the engine speed. Therefore the model accuracy was also calculated as the number of deviating engine cycles the absolute error resulted in. This calculation is described by equation (4.5), where the absolute error in seconds was divided with the cycle time t_{cycle} . The reason behind the minus sign in the equation is to obtain a positive value for the number of cycles when the estimated time is larger than the measured.

$$\Delta n_{cycles} = \frac{-\Delta t}{t_{cycle}}$$

$$t_{cycle} = \left(\frac{N_e [rpm]}{60 * 2} \right)^{-1}$$

$$\Delta n_{cycles} = -\Delta t \frac{N_e [rpm]}{120} \quad (4.5)$$

Figure 4.15 presents the number of deviating engine cycles the estimation error causes for model (3.46) that describes the transport delay between the long route EGR valve and the cylinders.

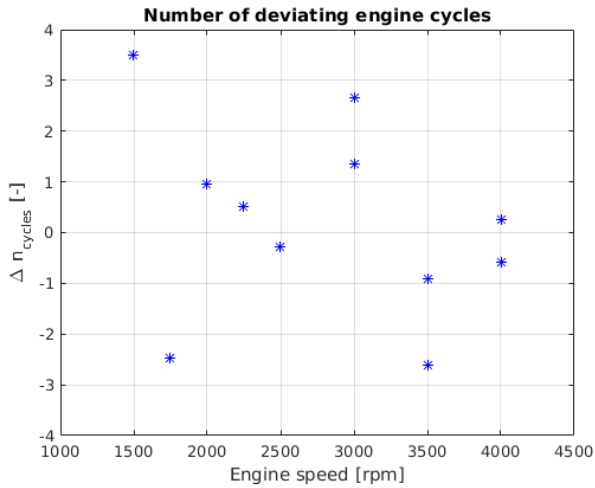


Figure 4.15: The number of cycles the estimation error results in. A positive number for Δn_{cycles} means that the recirculated gases enters the cylinders Δn_{cycles} cycles later than the estimated time, a negative value means that the gases enters the cylinders Δn_{cycles} cycles before the estimated time. Data points 2,4,...,22 in Table 3.3 were used for validation of the model, while data points 1,3,...,23 were used for modeling.

4.4.2 Time delay simulations in Simulink

In this section, the complete engine model with the long route EGR system implemented is simulated with different circumstances and compared to measurements from the engine rig.

Measurements from the engine rig when a step is made in the long route EGR valve at relative low engine speed and at low load (1500 rpm and 1.0 gram air per engine revolution), are presented in figure 4.16 and 4.17.

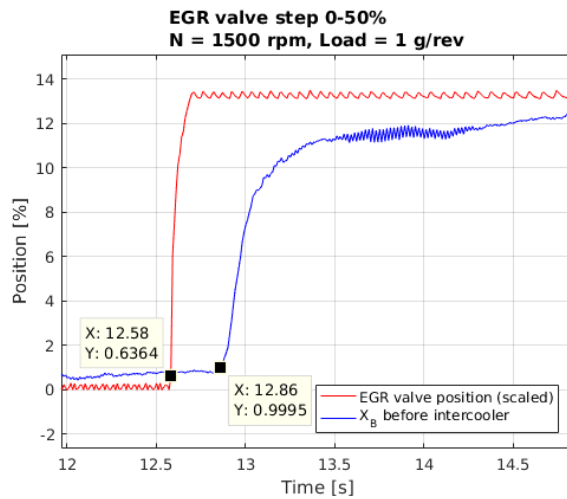


Figure 4.16: The burned gas fraction between the compressor and inter-cooler when a step is made in the long route EGR valve from 0% to 50%. The burned gas fraction in this figure is calculated from the oxygen level and MAF-sensor. The EGR valve position has been scaled.

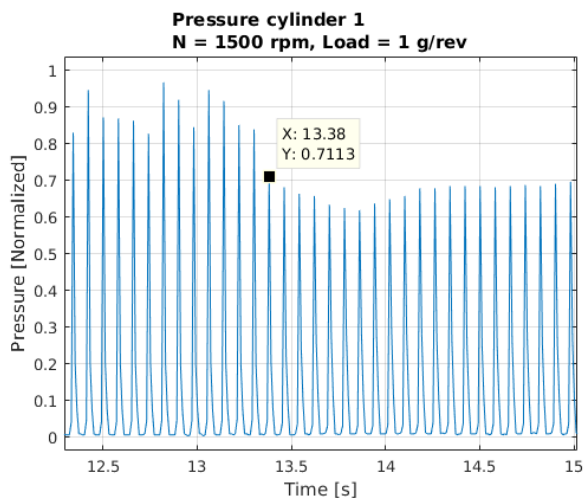


Figure 4.17: Pressure in cylinder number one. Since the recorded data was not processed to present the actual pressure, the signal was normalized since the characteristics is clear anyway. The cylinder pressure decreases when the recirculated exhaust gases reaches the cylinders.

A simulation without the transport delay model is presented in figure 4.18. The burned gas fraction starts to increase almost immediately after the step is made in figure 4.18. Figure 4.19 presents the simulated result for the same operating point but with the transport delay modeling.

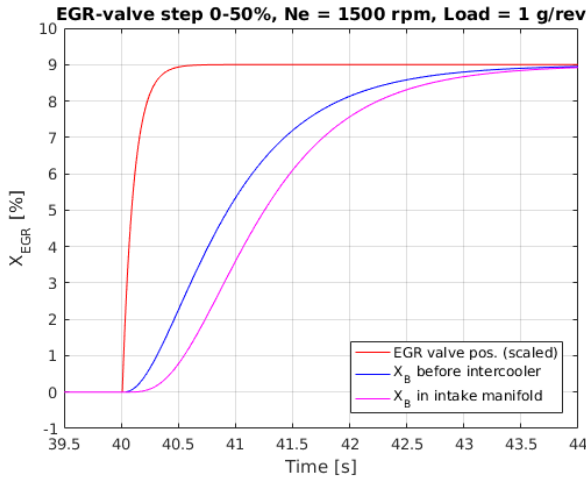


Figure 4.18: Simulation of the complete engine model with the long route EGR systems and gas mixture models implemented, but without transport delay models for the recirculated exhaust gases. A step is made in the long route EGR valve at $t = 40$ seconds. The burned gas fraction starts to increase almost immediately after the step is made.

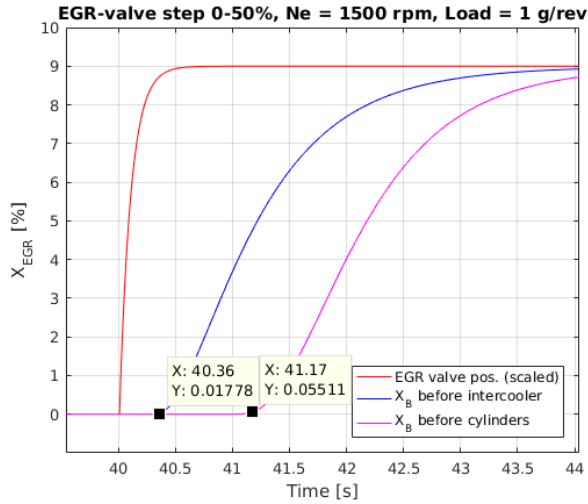


Figure 4.19: Simulation of the complete engine model with the long route EGR systems and gas mixture models implemented with transport delay modeling for the recirculated exhaust gases. A step is made in the long route EGR valve at $t = 40$ seconds.

Measurements from the engine rig when a step is made in the long route EGR valve at an operating point with higher engine speed and higher load (3000 rpm and 1.5 gram air per engine revolution), is presented in figure 4.20 and 4.21.

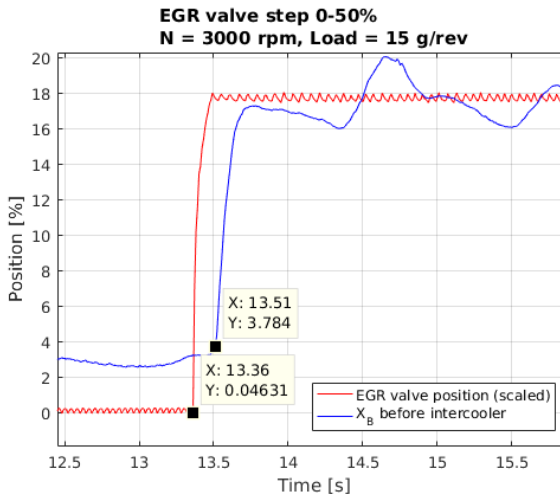


Figure 4.20: The burned gas fraction between the compressor and intercooler when a step is made in the long route EGR valve from 0% to 50%. The burned gas fraction in this figure is calculated from the oxygen level and MAF-sensor. The EGR valve position has been scaled.

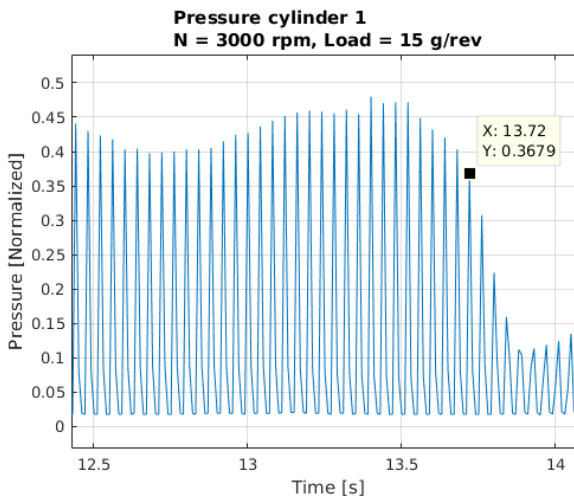


Figure 4.21: Pressure in cylinder number one. Since the recorded data was not processed to present the actual pressure, the signal was normalized since the characteristics is clear anyway. The cylinder pressure decreases when the recirculated exhaust gases reaches the cylinders.

The simulated step at the same operating point is presented in figure 4.22.

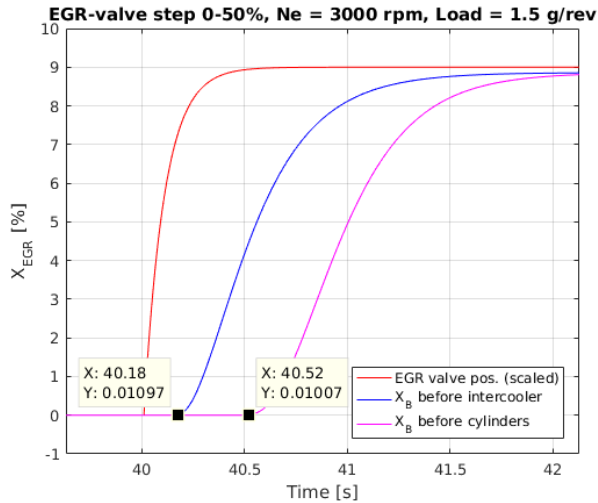


Figure 4.22: Simulation of the complete engine model with the long route EGR systems and gas mixture models implemented with transport delay modeling for the recirculated exhaust gases. A step is made in the long route EGR valve at $t = 40$ seconds.

Measurements from the engine rig when a step is made in the long route EGR valve at an operating point with even higher engine speed (4000 rpm and 1.5 gram air per engine revolution), is presented in figure 4.23 and 4.24. The simulated step at the same operating point is presented in figure 4.25.

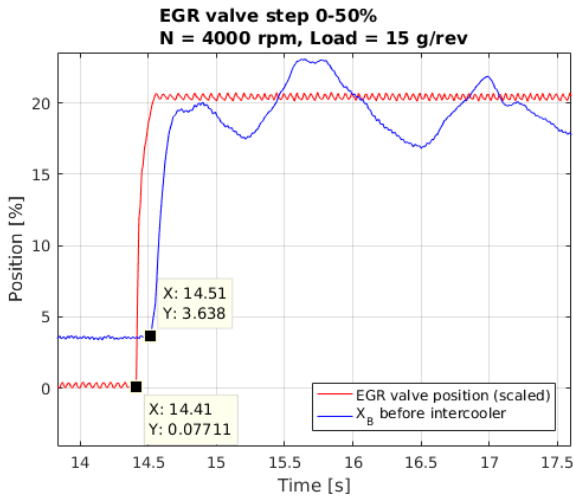


Figure 4.23: The burned gas fraction between the compressor and intercooler when a step is made in the long route EGR valve from 0% to 50%. The burned gas fraction in this figure is calculated from the oxygen level and MAF-sensor. The EGR valve position has been scaled.

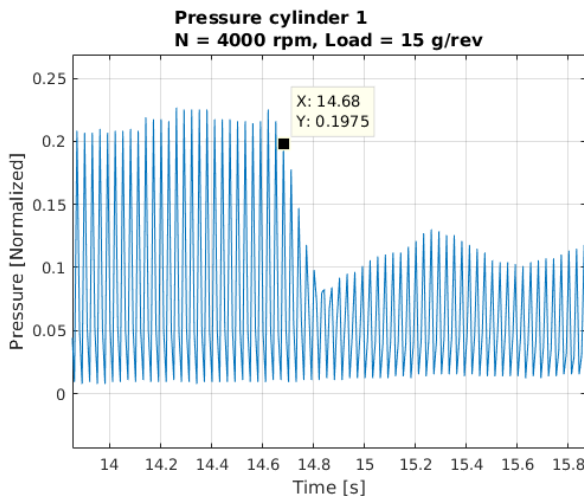


Figure 4.24: Pressure in cylinder number one. Since the recorded data was not processed to present the actual pressure, the signal was normalized since the characteristics is clear anyway. The cylinder pressure decreases when the recirculated exhaust gases reaches the cylinders.

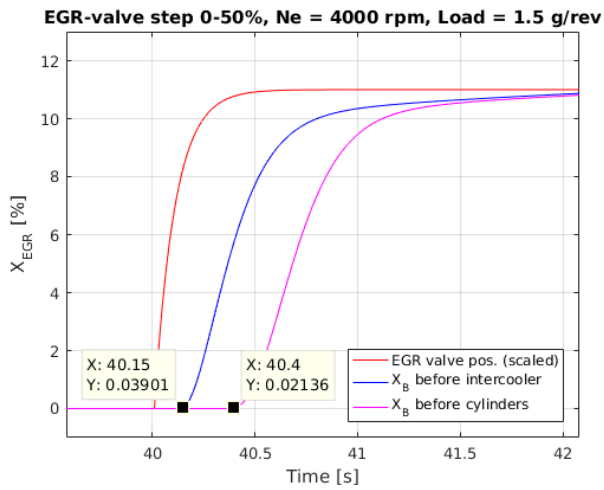


Figure 4.25: Simulation of the complete engine model with the long route EGR systems and gas mixture models implemented with transport delay modeling for the recirculated exhaust gases. A step is made in the long route EGR valve at $t = 40$ seconds.

The transport delays observed in the measurement for the operating points simulated above is presented in table 4.1. The transport delay calculated from the transport delay models for the corresponding operating points are presented in table 4.1.

Table 4.1: Measured transport delay from the long route EGR valve to the O_2 -sensor and to the cylinders. The engine speed and load is presented in table 3.3 for each data point.

Data point	Measured delay EGR valve to O_2 -sensor	Measured delay EGR valve to cylinders
2	0.28	0.80
14	0.15	0.36
22	0.10	0.27

Table 4.2: Modeled transport delay from the long route EGR valve to the O_2 -sensor and to the cylinders. The values in this table are calculated out from the parameterised models (3.44) and (3.46). The engine speed and load is presented in table 3.3 for each data point.

Data point	Modeled delay EGR valve to O_2 -sensor	Modeled delay EGR valve to cylinders
2	0.29	0.93
14	0.14	0.40
22	10	0.30

Table 4.3: Simulated transport delay from the long route EGR valve to the O_2 -sensor and to the cylinders. The values are calculated out from figure 4.19, 4.22 and 4.25. The engine speed and load is presented in table 3.3 for each data point.

Data point	Simulated delay EGR valve to O_2 -sensor	Simulated delay EGR valve to cylinders
2	0.36	1.17
14	0.18	0.52
22	0.15	0.4

5

Discussion and Conclusion

5.1 Model of the long route EGR system

The outcome for the validation of the MVEM models made clear which restriction model that fitted best. The exception might be the restriction models for the first catalyst brick. The accuracy of the restriction models could be further improved by parameterizing the models with more data points. Collecting static data points for parameterizing the mean value engine models is time consuming since the measured temperatures often takes long time to reach their steady points. As usual, the time available for the thesis work has limited the extent of the work sometimes.

The complete Simulink model with the long route EGR system, gas mixture model and transport time models implemented was able to simulate the characteristics of an engine with a long route EGR system. The models for calculating the transport delays were parameterized with all the collected data points when they were implemented in Simulink. However, the simulated transport delays were a bit higher than the measured and calculated value. This probably depends on the dynamics that exists in the control volume models, the concentration in each control volume has to be built up before the concentration in the next control volume model starts to increase. Even though the the dynamics are quite fast, it becomes added upon the calculated time delays modeled with time delay blocks. Another source to this could be that the modeled time is calculated from simulated values. If there is a model error on the intake side in the engine model, this will affect the simulated time delays.

The simulated static levels for the burned gas fractions also differs from the measured values. This probably depends on that the EGR valve model that simulates the mass flow over the EGR circuit generally gives a lower value than the measured values with the oxygen sensor, see figure 4.9. Another source could be that the engine model in Simulink does not take fuel enrichment for cooling into account, the simulated temperatures in the catalyst can differ a lot compared to the measured values. This can affect the results from simulations with the long route EGR system. For the EGR valve model in this work, the temperature used was the temperature that was measured just before the long route EGR intercooler. The temperature used in the Simulink model, was the temperature between the catalyst bricks, that might differ a bit from the temperature just before the intercooler due to heat exchange to the surrounding environment for the short pipe between the catalyst and long route EGR intercooler. This problem can probably be solved by separating the temperature drop for the pipe between the catalyst and long route intercooler from the temperature drop in the intercooler, by adding an additional model for the temperate drop in the pipe.

Another thing that was observed from the measurements was that the static value burned gas fraction was not equal to zero when the EGR valve was closed. The reason may be the gases from the crankcase ventilation that was led in to the pipe before the oxygen sensor, or that oscillations in the EGR valve position when the position controller was switched on, caused some leakage through the valve.

5.2 Different methods of estimating the mass flow over the long route EGR circuit

The comparison of the different estimation methods for the mass flow over the long route EGR circuit, see figure 4.9, showed that estimating the EGR mass flow from the modeled cylinder mass flow gave similar result to the mass flow estimated from the oxygen sensor. The mass flow estimated from the EGR valve model generally gave a lower mass flow than the two other methods. For the throttle valve in this work, estimating the mass flow by measuring the oxygen or estimating the cylinder mass flow is most likely more accurate than estimating the mass flow from the pressure drop over the EGR valve. However, the exact accuracy of the models is not known. But since two of the methods has a small deviation compared to the method where the mass flow is estimated from the pressure difference over the valve, it is more likely that the actual value is closer to the estimations from the two other methods.

Based on the conclusion above, the mass flow modeled from the modeled mass flow into the cylinders seems to perform as well as estimating the mass flow from the oxygen sensor. How the methods perform under transients, for example under a pressure build-up in the intercooler, would need to be further investigated.

5.3 Proposed control strategy for the long route EGR system

If the transport delay models presented under 3.4 would be accurate enough for control of the engine, and work satisfactory under transients, one method to control the long route EGR valve, would be to use a feed-forward controller based on a throttle model or a look-up table. Since the validation of the EGR valve model in this work, see figure 4.8 under 4.1, does not seem to give a very accurate result, a feedback controller will most likely be needed. Using a lambda sensor as feedback might be difficult, since it changes its output over time when it is used in the prevailing temperature in the engines air intake system. Therefore it might be hard to use such sensors for production vehicles. But since the estimation of the EGR mass flow from the modeled mass flow into the cylinders, seems to give similar results as when estimating the EGR mass flow from the oxygen sensor, the feedback controller could be based on the mass flow calculated from equation 3.36. However, since the comparison of the methods is only made under steady operating points, the dynamic of the estimation methods would need to be further studied, and would need to be modeled or mapped if the feedback controller has to be gain scheduled.

In case the transport delay model would turn out to be too inaccurate for controlling the engine, an oxygen sensor could be placed in the intake manifold. The issue here is that the lambda sensor has problem with the prevailing temperatures, and the SiC-FET sensor is not yet fully developed, and mass production of SiC-FET sensors would be many years ahead.

5.4 Future work

For the Simulink model, this work could be continued with collecting more data points for parameterizing the MVEM models. The accuracy for mass flow over the long route valve in the Simulink model could probably be increased by implementing separate models for the temperature drop in the pipe between the catalyst and EGR intercooler and the temperature drop over the EGR intercooler. Then the temperature used for the throttle valve model would correspond more to the actual position on the engine rig. Another alternative would be to recalculate the effective area in the EGR valve model and use the temperature and pressure between the EGR intercooler and EGR valve.

The accuracy of the transport delay models during transients could also be studied, for example how the models performs during a pressure build up or pressure drop in the boost pressure, or a quick change in engine speed or engine load. Dynamic studies of the different methods of estimating the mass flow over the long route EGR system, described under section 3.3, would also need to be further studied.

The work could also be continued with developing and implementing a controller for the burned gas fraction in the engines air intake system. For that work, the Simulink models developed in this work, hopefully could be an aid for testing the controllers in a simulation environment.

Bibliography

- [1] Author Andersson, Mike, Author Lloyd Spetz, Anita, Author Pearce, Ruth, kemi och biologi Tillämpad sensorvetenskap Originator Linköpings universitet, Institutionen för fysik, and Originator Linköpings universitet, Tekniska högskolan. *Recent trends in Silicon Carbide (SiC) and Graphene based gas sensors*, page 117. Woodhead Publishing Limited. ISBN 978-0-85709-236-6. Cited on pages 4 and 8.
- [2] Lars Eriksson and Lars Nielsen. *Modeling and control of engines and drivelines*. Chichester : Wiley, 2014, 2014. ISBN 9781118479995. Cited on page 11.
- [3] J.G. Hawley, F.J. Wallace, A. Cox, R.W. Horrocks, and G.L. Bird. Reduction of steady state nox levels from an automotive diesel engine using optimised vgt/egr schedules. Cited on page 1.
- [4] John B. Heywood. *Internal combustion engine fundamentals*. McGraw-Hill series in mechanical engineering. New York : McGraw-Hill, cop. 1988, 1988. ISBN 007028637X. Cited on page 1.
- [5] Hyunjun Lee, Yeongseop Park, Seungwoo Hong, Minkwang Lee, and Myoungho Sunwoo. Egr rate estimation for cylinder air charge in a turbocharged diesel engine using an adaptive observer. In *SAE Technical Paper*. SAE International, 04 2013. Cited on page 4.
- [6] F. Liu and J. Pfeiffer. Estimation algorithms for low pressure cooled egr in spark-ignition engines. *SAE International Journal of Engines*, 8(4). ISSN 19463944. Cited on page 4.
- [7] Lennart Ljung and Torkel Glad. *Modellbygge och simulering*. Lund : Studentlitteratur, 2004, 2004. ISBN 9144024436. Cited on page 4.
- [8] J.M. Luján, H. Climent, R. Novella, and M.E. Rivas-Perea. Influence of a low pressure egr loop on a gasoline turbocharged direct injection engine. *Applied Thermal Engineering*, 89:432–443, 2015. ISSN 13594311. Cited on page 3.

- [9] Ingemar Lundström, Hans Sundgren, Fredrik Winquist, Mats Eriksson, Christina Krantz-Rülcker, and Anita Lloyd-Spetz. Twenty-five years of field effect gas sensor research in linköping. *Sensors Actuators: B. Chemical*, 121 (Special Issue: 25th Anniversary of Sensors and Actuators B: Chemical):247 – 262. ISSN 0925-4005. Cited on page 8.
- [10] Per Öberg. *A DAE Formulation for Multi-Zone Thermodynamic Models and its Application to CVCP Engines*. PhD thesis, Linköpings universitet, 2009. Cited on page 3.
- [11] Vitek Oldřich, Macek Jan, Macek Jan, Polášek Miloš, Polášek Miloš, Schmerbeck Stefan, and Kammerdiener Thomas. Comparison of different egr solutions. Cited on page 3.
- [12] Youngsoo Park and Choongsik Bae. Experimental study on the effects of high/low pressure egr proportion in a passenger car diesel engine. *Applied Energy*, 133:308 – 316. ISSN 0306-2619. Cited on page 3.
- [13] Junting Qiu. Modeling, simulation and control of long and short route egr in si engines. Master's thesis, Linköpings universitet, SE-581 83 Linköping, 2015. Cited on pages 3 and 4.
- [14] Ulrica Renberg. 1d engine simulation of a turbocharged si engine with cfd computation on components. Cited on page 4.
- [15] Konstantinos Siokos, Rohit Koli, Robert Prucka, Jason Schwanke, and Julia Miersch. Assessment of cooled low pressure egr in a turbocharged direct injection gasoline engine. *SAE International Journal of Engines*, (4), 2015. ISSN 1946-3944. Cited on page 3.
- [16] Johan Wahlström and Lars Eriksson. Modelling diesel engines with a variable-geometry turbocharger and exhaust gas recirculation by optimization of model parameters for capturing non-linear system dynamics. *Proceedings of the Institution of mechanical engineers. Part D, journal of automobile engineering*, page 960. Cited on page 3.
- [17] Haiqiao Wei, Tianyuand Zhu, Gequnand Shu, Linlinand Tan, and Yuesen Wang. Gasoline engine exhaust gas recirculation - a review. *Applied Energy*, 99:534 – 544, 2012. Cited on page 3.